An empirical formula to assess ultimate strength of initially deflected plate: Part 2 = Combined longitudinal compression and lateral pressure

Do Kyun Kim [a, b*], Shen Li [c], Kwangkyu Yoo [d], Kumutha Danasakaran [e], and Nak-Kyun Cho [f *]

[a] Department of Naval Architecture and Ocean Engineering, College of Engineering, Seoul National University, Seoul, South Korea

[b] Research Institute of Marine Systems Engineering, Seoul National University, Seoul, Korea

[c] Department of Naval Architecture, Ocean and Marine Engineering (NAOME), University of Strathclyde, Glasgow, United Kingdom

[d] Department of Aeronautics, Imperial College London, London, UK

[e] Ocean and Ship Technology (OST) Research Group, Department of Civil and Environmental Engineering, Universiti Teknologi PETRONAS, Seri Iskandar, Perak, Malaysia

[f] Department of Manufacturing Systems and Design Engineering, Seoul National University of Science and Technology, Seoul, South Korea

Abstract

This study proposes an empirical formula to predict the ultimate strength of the initially deflected plate subjected to combined longitudinal compression and lateral pressure. The reliable plate scenarios selected are analysed by the ALPS/ULSAP (= Analysis of Large Plated Structures/Ultimate Limit State Assessment Program) method. In total, 5,600 plate scenarios, including the effects of geometry, material and applied load properties, are generated and used as input data for structural analysis to obtain the ultimate strength of the plates. In particular, five water depths (h) cases (i.e., 0, 5, 10, 15, and 20 m), four material yield strength (i.e., 235, 275, 315, and 355MPa) and various initial deflection amounts were considered together with the wide range of geometric properties. The empirical formula obtained shows good agreement with ALPS/ULSAP simulation results (R^2 = 0.994). The applicability of the outcome verified by statistical analysis and the effect of individual parameters considered on the ultimate strength of the plate is documented. The valuable examples are also provided with a detailed user guide. The obtained result may help estimate the ULS characteristic of the plate under combined compression and lateral pressure. Also, it can be used as a practical design guide for the robust design of the ship's plate.

**Corresponding authors: Do Kyun Kim (do.kim@snu.ac.kr) and Nak-Kyun Cho (nkcho@seoultech.ac.kr).*

Keywords: *Uimitate limit state, initial deflection, plate, ships and offshore structures, health monitoring, lateral pressure*

1. Introduction

1.1 Limitation of the previous study

Ship structures are continuously exposed to complex and harsh environmental conditions during their design life, which is about 20-25 years based on the common structural rule (CSR) for commercial ships IACS (2006a, 2006b). This means that we need a safer and robust design, and the design criteria are gradually improving from working stress design (WSD) to the limit state design (LSD) (Paik et al., 2009). In general, the LSD divides into the Ultimate Limit State (ULS), the Fatigue Limit State (FLS), the Accident Limit State (ALS), and the Serviceability Limit State (SLS) (Paik, 2018), which we consider only the ULS aspects in the present study.

Design rules by classification societies offer in simple empirical forms based on their long-established know-how and experience. They tend to utilise detailed FEM and CFD techniques in complex or specific cases. Of course, FEM and CFD techniques are improving their accuracy through comparative verification with ongoing experiments.

In ship structures, compression and tensile loads are repeatedly applied to the mid-ship section, especially the deck and bottom, due to the influence of vertical bending moments throughout the operation. In particular, the ultimate strength evaluation of the abovementioned structures is one of the main concerns for ship structural designers in the design stage. The primary structural members of the ship include local structural elements such as unstiffened panel (= plate), stiffened panel, and others. These local structural elements are considered an important role in the buckling phenomenon.

The local strength assessment should consider evaluating the actual safety level by identifying the applied action (= loads or demand) and action effect (= structural capacity) to the local element. This study considers applied action, i.e., combined axial compressive forces and lateral pressure. At the same time, the ultimate strength of the plate is only targeted as a structural capacity that the proposed empirical formula can predict by this study.

Researchers have conducted various studies to estimate the ultimate strength capacity of a single-loaded unstiffened and stiffened structure, i.e. longitudinal compression, by

experimental (Chen et al., 2004; Faulkner, 1977; Gordo and Soares, 2008; Kim et al., 2021; Kong et al., 2020; Manuel Gordo and Guedes Soares, 2011; Paik et al., 2020; Shanmugam et al., 2014; Xu and Soares, 2012), numerical (Fujikubo et al., 2005; Georgiadis et al., 2021; Kim et al., 2022; Li et al., 2021b; Liu et al., 2020; Paik et al., 2008a, b, c; Paik et al., 2009; Paik and Seo, 2009a, b; Ringsberg et al., 2021), empirical (Li et al., 2021a)and analytical methods (Benson et al., 2015; Brubak et al., 2013; Chen, 2003; Li et al., 2019). In particular, Paik (2018), Yao and Fujikubo (2016a), Hughes and Paik (2010) provided well-established knowledge to understand the complex structural behaviour of ships and offshore structures in the ultimate limit state (ULS).

Moreover, Cui and Mansour (1998); Faulkner (1975); Kim et al. (2018a); Lind et al. (1971); Zhang (2016) provided a wide range of technical reviews, which may help to understand the existing techniques to analyse and predict ULS of the local structural elements. In addition, ISSC may significantly contribute to developing the ultimate strength assessment of the ships and offshore structures (ISSC, 2009, 2012, 2015, 2018, 2022). Empirical formulas have also been developed, which are preferred due to their cost-effectiveness of computation time when engineers involve the pre-FEED work. In general, pre-FEED (Front End Engineering and Design) or conceptual design is considered a preliminary step taken prior to the main engineering work to confirm the economic and technical feasibility of the given project.

For example, predicting the ultimate strength of the plate (Kim et al., 2018b; Paik et al., 2004) and the stiffened panel (Khedmati et al., 2010; Kim et al., 2017; Kim et al., 2019a; Kim et al., 2020; Paik, 2007; Paik and Thayamballi, 1997) subjected to compression can be referred. Recently, Xu et al. (2018) proposed an empirical formula that considers various load combinations.

Various numerical analysis techniques, including FE modelling, boundary condition, etc., are suggested and verified (ISSC, 2012; Li and Kim, 2022; Paik et al., 2008a; Paik and Seo, 2009a). In addition, computational uncertainties of ultimate limit state assessment of ship structures (Li et al., 2021c), geometric imperfection effect (Li et al., 2022) and load-shortening curve prediction technique (Li et al., 2021a) are also recently investigated. Furthermore, various studies investigated the effect of lateral pressure and combined loads by many research groups (Jiang and Zhang, 2015; Khedmati et al., 2016; Ma and Wang, 2021; Ma et al., 2021; Xu et al., 2017).

With regards to the ultimate strength of the plate, several empirical formulas have been provided based on the effective-width concept through various studies over the past 150 years (AISC, 1961; BS153, 1966; BS499, 1961; Carlsen, 1977; Chilver, 1953; Cox, 1933; Cui and Mansour, 1998; Dwight and Moxham, 1969; Faulkner, 1975; Frankland, 1940; Gerard, 1957; Hughes, 1983; Ivanov and Rousev, 1979; Marguerre, 1937; Paik, 2008; Paik et al., 2004; Schnadel, 1930; Sechler, 1933; Smith et al., 1988; Soreide and Czujko, 1983; Timoshenko, 1936; Ueda et al., 1986; Ueda et al., 1992; Ueda et al., 1975; von Kármán, 1924; Winter, 1940). From the past and continued research outcomes, it can be concluded that the empirical formula technique is practical and can widely be adopted in ships and offshore industries.

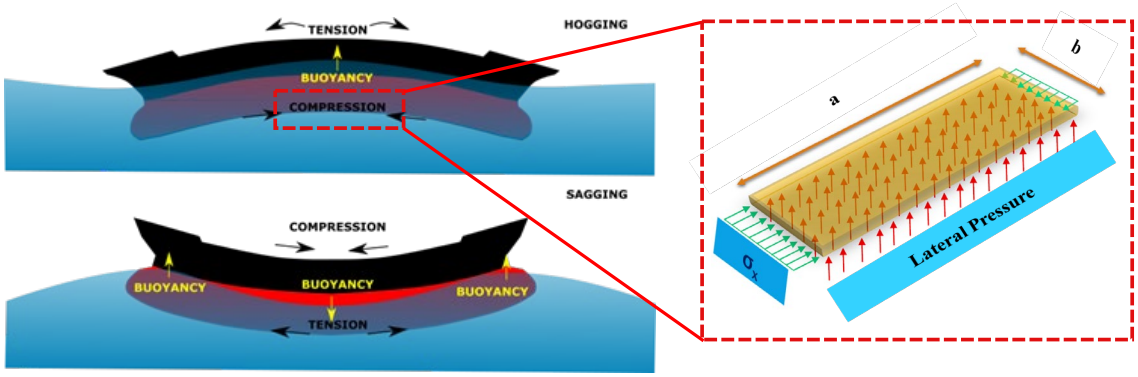

Fig. 1. *Schematic view of the plate at outer bottom subjected to axial compression and lateral pressure (Lim, 2018).*

The development of the empirical formula may support the structural designer in predicting the intact or damaged structural health condition, and various studies were conducted by considering a difference in the target structure, model extent, applied load, expected result, modelling, analysis techniques, etc. This study can also be considered as one of the research categories to assess the condition of the structures, which may provide relevant and direct ways, i.e., simplified diagrams or empirical formulas, to understand the actual structural health condition.

1.2 Problem statement, objectives and scope of this study

Among other empirical formulas, recently, Kim et al. (2018b) developed an empirical formulation technique that can predict the ultimate strength of the initially deflected plate under longitudinal compression. Their research considered the initial deflection of buckling

shape (see Eq. 2.1) and provided a precise empirical formula for changes in initial deflection amount by determining the sub-coefficients. It was an advanced empirical formula but limited to a longitudinally compressed plate, considered a deck plate.

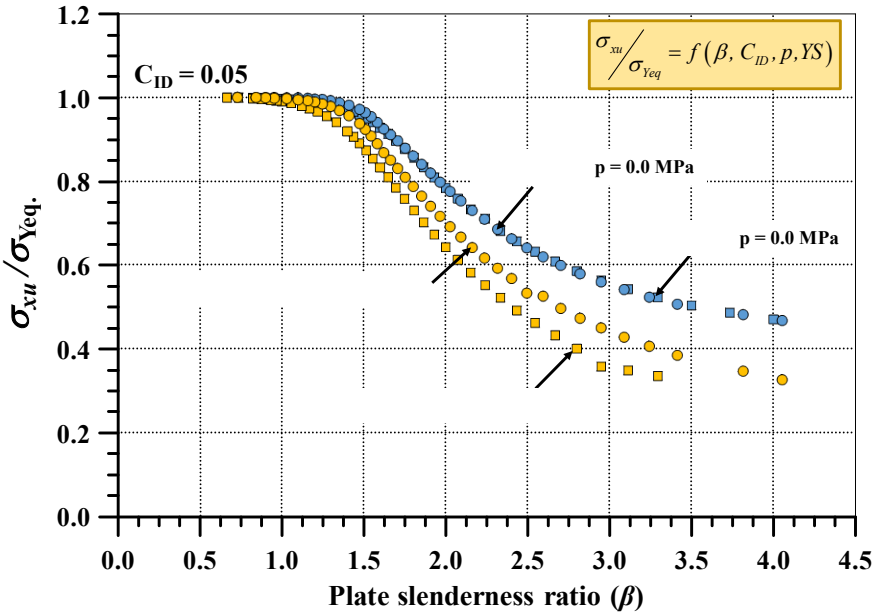

Fig. 2. *Example of the ultimate limit state or ultimate strength computation results (Note: C_{ID} = initial deflection coefficient to present the amount; p = lateral pressure, YS = yield strength).*

In this regard, we expand scenarios by considering the effect of lateral pressure, as presented in Figure 1. Also, we recognised that the ultimate strength capacity varies as lateral pressure increases, as shown in Figure 2. In particular, the effect of material yield strength should also be taken into account to understand the ultimate strength characteristic of the plate under combined longitudinal compression and lateral pressure.

Therefore, a refined empirical formula will be proposed in this study by considering the effect of plate slenderness ratio (b), initial deflection coefficient (C_{ID}), lateral pressure (p) and material yield strength (s_Y). In total, 5,600 cases of the scenarios are generated by considering the above four parameters.

The following scopes aim to be targeted by this study, and the advantage and limitations of the present study will clearly be summarised in the conclusion part.

- *Effect of material yield strength*

- *Effect of initial deflection level*
- *Providing empirical formulation with its applicable range*

2. Methodology

2.1 Limitation of the existing formula

The recently proposed general shape of the empirical formulation by Kim et al. (2018b) is shown in Eq. (1).

$$\frac{\sigma_{xu}}{\sigma_Y} = 1 - \exp\left(-0.9025\left(\frac{c_1}{\beta} + \frac{c_2}{\beta^2} + \frac{c_3}{\beta^3} + c_4\right)\right) \qquad \text{Eq. (1)}$$

where σ_{xu} *= ultimate strength of plate,* σ_Y *= material yield strength,* β *= plate slenderness ratio (=* $\frac{b}{t}\sqrt{\frac{\sigma_Y}{E}}$*),* b*= plate width or breadth,* t *= plate thickness,* E *= Elastic modulus,* c_1 *to* c_4 *= sub-coefficients to consider initial deflection effect.*

The advantage of Eq. (1) is that the single formula, not dividing the range, is able to capture accurate ultimate strength behaviour. Most of the existing formulas predict the ultimate limit state (σ_{xu} / σ_Y *) based on the plate slenderness ratio range. In general, ULS (=* σ_{xu} / σ_Y *) remains as 1.0 as* β *increased by certain values, i.e., 1.9 for von Kármán (1924) and 1.0 for Faulkner (1975) in the first range. The ULS will then tend to decrease. At this point, Kim et al. (2018b) stressed that the ultimate strength tends to decrease smoothly by comparing with the nonlinear finite element method (NLFEM), and they proposed a single formula as shown in Eq. (1). In addition, any amount of the initial deflection, based on the buckling mode shape shown in Eq. (2.1), can be considered.*

They adopted the three initial deflection levels, including slight, average, and severe conditions presented in Eq. (2.2), and four additional levels were considered, as shown in Eq. (2.3).

General expression of buckling mode shape initial deflection of the entire plate in longitudinal compression

$$w_{opl} = A_{om} \times \sin\left(\frac{mpx}{a}\right) \times \sin\left(\frac{py}{b}\right) \qquad \text{Eq. (2.1)}$$

Maximum initial deflection levels (Smith et al., 1988)

$$A_{om} = \begin{cases} 0.025 b^2 t & \text{for slight level} \\ 0.1 b^2 t & \text{for average level} \\ 0.3 b^2 t & \text{for severe level} \end{cases} \qquad \text{Eq. (2.2)}$$

where, maximum initial deflection can be obtained at the centre of the plate $(x = a/2, y = b/2)$, *which means that* $w_{opl} = A_{om}$ *in this case.*

Regarding the adopted maximum initial deflection of the plate, the equation proposed by Smith et al. (1988) shown in Eq. (2.2) is based on full-scaled measurement, which is close to a hungry-horse mode. With regards to the level of the initial deflection shown in Eq. (2.2), the maximum deflection level may be adjusted if we consider the modern ships from the improvement of fabrication procedure and quality control system. However, the wide range of the initial deflection levels is considered by assuming Smith's equation for academic research purposes.

The buckling mode shape adopted in this study may underrate the ultimate strength capacity due to a more significant deflection developed during the progressive collapse. However, buckling mode is often applied in ships and offshore industry to analyze by an analytical or semi-analytical method for the practical design purpose with the advantage of mathematical simplicity by presenting sinusoidal function. This is discussed again in section 4.2.3 in this study.

Expression of deflection amplitude

$$w_{opl} \left(= A_{omn}\right) = C_{ID}\, b^2 t \qquad \text{Eq. (2.3)}$$

$$\text{where, } C_{ID} = \text{initial deflection coefficient} = \begin{cases} = 0.025 \\ = 0.05 \\ = 0.1 \\ = 0.15 \\ = 0.2 \\ = 0.25 \\ = 0.3 \end{cases}.$$

The formula in Eq. (1) consists of four sub-coefficients (c_1-c_4), including the plate slenderness ratio (β). Kim et al. (2018b) proposed additional sub-functions by investigating the relationship between c_1-c_4 and initial deflection coefficient (C_{ID}). Details may be referred to Kim et al. (2018b), and its applicability and accuracy were validated by Salazar-Domínguez et al. (2021). It is recommended to estimate the ultimate strength of the initially deflected plate under longitudinal compression conditions.

However, the empirical formula has a disadvantage that can only be applied under longitudinal compression. This study proposes an empirical formula that can be used under combined load, i.e., longitudinal compression and lateral pressure.

2.2 Procedure to develop an empirical formula

Figure 3 illustrates the general procedure to develop an empirical formula. The present study will follow the steps given in Fig. 3 to propose the empirical formula to predict the plate's ultimate strength under combined longitudinal compression and lateral pressure.

2.2.1 Definition of Input data [Step 1]

As a first step to run the processing toolbox illustrated in Fig. 3, which will provide an empirical formula at the end, initial input data should be defined. It can be categorised into three such as geometric and material properties and loading conditions. In the case of geometric property, The plate is a simple 2D structure defined by plate length (a), plate width or breadth (b), and plate thickness (t). Besides, the material stress-strain curve should also be needed, in general. The ultimate strength of structures is affected by material properties, while designers tend to reduce the safety-related uncertainties. Therefore, a perfectly bi-linear stress-strain curve with zero tangential angles, which consists of elastic modulus (E) and material yield strength (σ_Y), is adopted.

In addition to geometric and material properties, applied loading type should also be clearly defined. This study aims to propose an empirical formula in predicting the ultimate strength of the plate under combined longitudinal compression (σ_x) and lateral pressure (p).

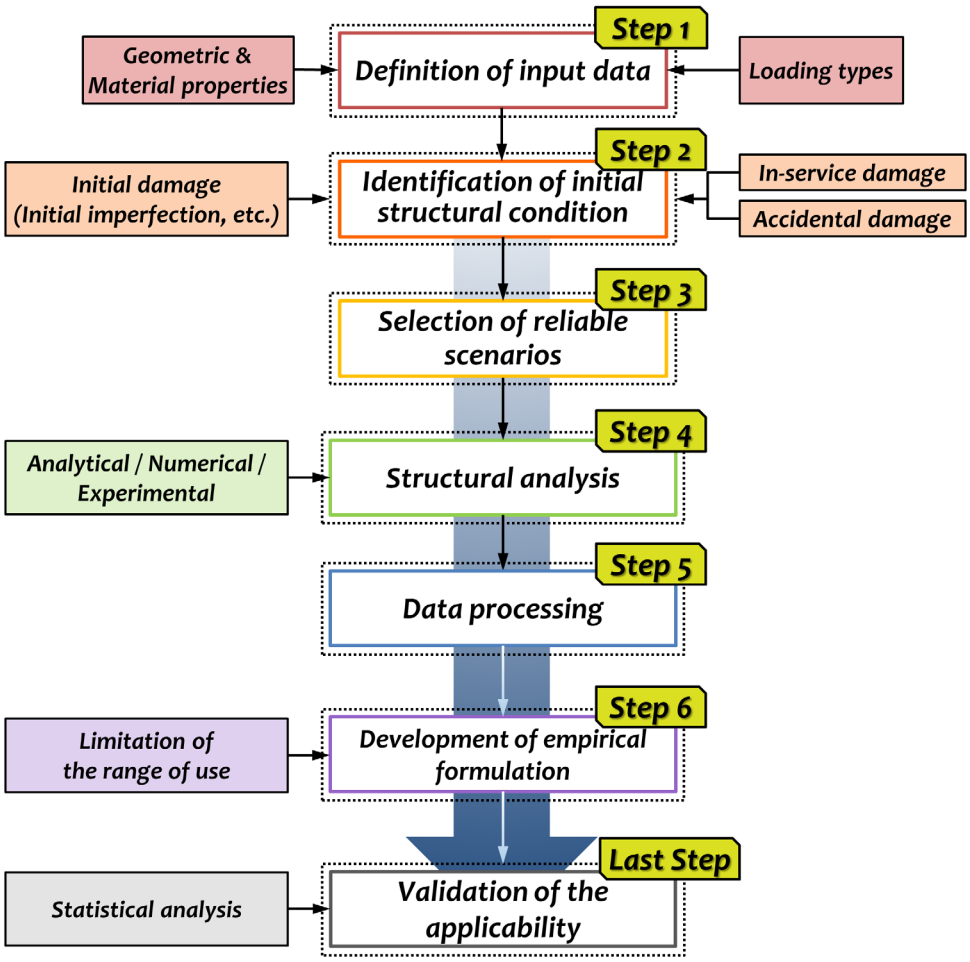

Fig. 3. *The general procedure in developing the empirical formula.*

2.2.2 *Identification of initial structural condition [Step 2]*

The general procedure for condition assessment of structure suffered by accidental and in-service damage is proposed by Kim (Kim, 2013). It is not precisely a similar procedure, but identifying the initial structural condition is essential to conduct structural analysis. Therefore, initial deflection is considered an initial structural condition, and the buckling mode shape initial deflection effect presented by sinusoidal function is only adopted in this study. In the case of welding-induced and pressure loading-induced residual stress effects have not been considered. From the previous investigation by Khan and Zhang (2011), 10 to 13% of ultimate strength differences may be caused by residual stress. Details on the effect of initial imperfection, such as initial deflection shape, residual stress, etc., may be referred to (Cui and Mansour, 1998; Guedes Soares, 1988; Khan and Zhang, 2011; Li et al., 2021b; Paik et al., 2004; Raviprakash et al., 2012; Sadovský et al., 2005; Ueda et al., 1992; Yao and Fujikubo, 2016b).

2.2.3 Selection of scenarios [Step 3]

The scenarios applied to this study are summarised in Table 1. The plate length (a) and width (b) were fixed and changed the plate thickness (t_p), which may help to investigate the effect of plate slenderness ratio (β). Four types of materials (i.e., S235, S275, S315, S355 which represents the combination of structural steel material (S) and material yield strengths (235MPa, 275MPa, 315MPa and 355MPa)), and five lateral pressure conditions (p = 0, 0.05, 0.1, 0.15 and 0.2 MPa) were considered, along with seven levels of initial deflection (C_{ID} = 0.025, 0.05, 0.1, 0.15, 0.2, 0.25, 0.3). In this study, we conducted detailed investigations for a total of 5,600 analysis scenarios.

Table 1. Selected scenarios.

Material Properties	
Yield Strength (MPa)	235, 275, 315, 355
Elastic Modulus (GPa)	205.8
Poisson's Ratio	0.3
Geometrical properties (Unit = mm)	
Length (a)	4150
Breath (b)	830
Thickness (t_p)	40 cases (varies from 7 to 69mm) (To define the limitation, additional cases have been selected but it has not been counted.)
Initial deflection	
Initial deflection coefficient (C_{ID})	0.025, 0.05, 0.10,0.15,0.20, 0.25 0.30
Applied loads	
Lateral Pressure (MPa)	0, 0.05, 0.10,0.15, 0.20
Axial compression	Applied until structure collapse
$\underbrace{1}_{a} \times \underbrace{1}_{b} \times \underbrace{40}_{t}$ $\underbrace{7}_{C_{ID}}$ $\underbrace{4}_{\sigma_y} \times \underbrace{1}_{E}$ $\underbrace{5}_{p}$ = 5,600 scenarios geometric initial def. material lateral pressure	

2.2.4 Analysis method [Step 4]

The most significant advantage of a past study by Kim et al. (2018b) is that a reliable accuracy of empirical expression (R^2 = 0.99) is derived compared to 700 cases of ANSYS nonlinear finite element method (NLFEM) simulations, which carry additional computational cost than analytical or simplified design (= empirical formula) method. Moreover, the selected all scenarios in Table 1 are challenging to simulate by NLFEM. Therefore, we considered a semi-analytical method, named the ALPS/ULSAP method (ALPS/ULSAP, 2016), for the ultimate strength calculation of the plate in this study.

Paik and Seo (2009a) investigated the ultimate strength of unstiffened plate elements under combined biaxial thrust and lateral pressure using a nonlinear finite element approach with regard to numerical simulation techniques. The one-bay plate model was supported along four edges with no rotational constraint. It was analysed along with the 1/2+1+1/2 bay continuous plate model with the lateral deflection restrained by supporting members. The latter was subjected to rotational restraint along the plate edges under lateral pressure, as observed.

Paik (2018) mentioned that the rotational restraint significantly influenced the ultimate strength of plate elements under biaxial thrust under lateral pressure actions. The ALPS/ULSAP semi-analytical method captured this influence in the ultimate strength prediction with reasonable accuracy. Most studies on the ultimate strength of plates under longitudinal compression are related to plates having unrestrained edges that may lead to a zero net load in the transverse direction.

Basically, ALPS/ULSAP method evaluates the distribution of membrane stress inside a plate supported by stiffeners by nonlinear governing differential equations. The simply supported boundary condition for four plate edges is assumed. For the ULS assessment, ALPS/ULSAP method considers the plate's collapse when any part of the edges having been kept straight yields. The straight plate edge may no longer withstand the membrane-tension loads after the inception of yielding at the corresponding location of the plate edge (Paik and Seo, 2009a). Therefore, the following three conditions in Fig. 4 are evaluated to determine the ultimate strength of the plate by selecting the minimum value.

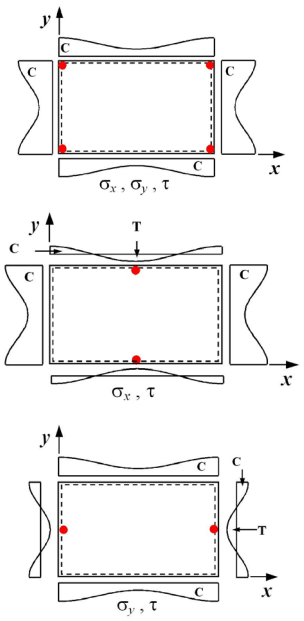

$$s_{eq1} = \sqrt{s_{x\max}^2 - s_{x\max}s_{y\max} + s_{y\max}^2 + 3t^2} = s_Y$$

$$s_{eq2} = \sqrt{s_{x\max}^2 - s_{x\max}s_{y\min} + s_{y\min}^2 + 3t^2} = s_Y$$

$$s_{eq3} = \sqrt{s_{x\min}^2 - s_{x\min}s_{y\max} + s_{y\max}^2 + 3t^2} = s_Y$$

(c) Plasticity at the transverse mid-edges

Fig. 4. *A brief introduction in determining the ultimate limit state of the plate by ALPS/ULSAP.*

In this regard, we employed ALPS/ULSAP semi-analytical method to cover the various scenarios represented in Table 1. The primary mechanism of how ALPS/ULSAP determine the ultimate strength of the plate is summarised in Fig. 4. It firstly checks plasticity conditions at the corners, longitudinal and transverse mid-edges. Secondly, calculate the equilibrium stress for the above three conditions, and finally, the minimum value will be selected as the ultimate strength of the plate. It means that ALPS/ULSAP considers relevant failure modes, and the ultimate strength will be selected based on the obtained lowest value. The ALPS/ULSAP may enable structural designers in predicting the ultimate strength of the local structural elements with effective computational cost. It is aware that PULS also provides a similar function in predicting ultimate strength values.

The accuracy validation and its application of the ALPS/ULSAP method have been conducted by several researchers (ISSC, 2009, 2012; Kim et al., 2014; Kim et al., 2015; Kim et al., 2012; Paik, 2018; Paik et al., 2008a; Paik and Seo, 2009a), so it will not discuss further.

2.2.5 Data processing [Step 5]

*Earlier in sections 2.1 and 2.2, we defined and discussed the input data (**Step 1**) and initial*

*imperfection identification (**Step 2**), scenario selection (**Step 3**), and analysis method (**Step 4**) applied to this study. Based on this, a total of 5,600 cases will be calculated by ALPS/ULSAP method.*

*The importance of data processing has been emphasised in recent years (Kim et al., 2019a; 2019b). At present, when diverse and vast amounts of data are pouring in, much attention is being paid to data processing techniques that efficiently and precisely analyse them and produce optimised results. Among them, the use of Artificial Intelligence (AI), including Machine Learning (ML) and Deep Learning (DL), is being highlighted. In addition, we also identify trends and derive empirical expressions through various existing probabilistic techniques (Wong and Kim, 2018). The obtained trend of ultimate strength capacity will be investigated as the plate slenderness ratio (β) increased so that the obtained data could be processed (**Step 5**).*

2.2.6 Development of empirical formula including its limitation [Step 6]

*In this work, we plan to propose empirical expressions based on the technique by Kim et al. (Kim et al., 2022). Additional effort has been made to derive a sub-formula that takes into account the effects of lateral pressure. The developed empirical formula may require verification of its scope of use (**Step 6**), and finally, a review of its applicability is required (**Step 7**).*

The empirical formula proposed in this study provided the most suitable fitting curve through the response surface method. The input included plate geometry (i.e., length, width, thickness), material property (yield strength, elastic modulus) and loading type (longitudinal compression and lateral pressure). The ultimate strength is given as a dimensionless value divided by the material yield strength.

2.2.7 Applicability of the proposed formula [Step 7]

The applicability of the developed formula should be evaluated. A detailed procedure to utilise the formula is also provided by covering the simple tutorial data in Section 4.

3. Development of empirical formula in predicting ultimate strength of the initially deflected plate under combined longitudinal compression and lateral

pressure

We remind us of the expected outcome of the empirical formula, which enables us to predict the ultimate strength of the plate under combined longitudinal compression and lateral pressure. On the other hand, the ultimate strength can be predicted once the plate's material, geometric, and loading properties are defined as the input data, as shown in Eq. (3).

$$ULS = f\left(\beta, C_{ID}, p, s_Y\right) \tag{3}$$

where, β *= Plate slenderness ratio (*$=\frac{b}{t}\sqrt{\frac{s_Y}{E}}$*);*

C_{ID} *= Coefficient of initial deflection;*

p *= Lateral pressure (MPa);*

s_Y *= material yield strength (MPa);*

In part 1 (Kim et al., 2022), the general shape of the empirical formula is proposed, as presented in Eq. (4).

$$\frac{s_{xu}}{s_Y} = 1 - \left\{C_1 \tan^{-1}\left(C_{ID} \times \left(\beta - C_{ID}\right) \times e^{C_2 C_3 \times \beta + \frac{1}{C_{ID} C_4}}\right)\right\}^6 \tag{4}$$

where, c_1 *to* c_4 *= coefficients, which varies in assumed condition.*

In part 1, they (Kim et al., 2022) conducted research to estimate the ultimate strength of the initially deflected plate subjected to longitudinal compression. They provided a generalised form of the empirical formula, which can be considered an extension of the research conducted by Kim et al. (Kim et al., 2018b). The empirical formula consists of three key variables, such as the plate slenderness ratio (β*), initial deflection coefficient (*C_{ID}*), and an additional four undecided coefficients (*c_1 *to* c_4*), as shown in Eq. (4). They expressed the normalised ultimate strength (*s_{xu}/s_Y*) that can be formulated as a function of plate slenderness ratio and initial deflection coefficient (*$= f\left(\beta, C_{ID}\right)$*).*

In this study, we consider two more variables, such as lateral pressure (p*) and material yield*

strength (s_Y), as shown in Eq. (3). Those two variables need to be incorporated with coefficients (c_1 to c_4) if we want to adopt Eq. (4) by not revising the general shape. Therefore, the relationship between coefficients (c_1 to c_4) and two additional variables (p and s_Y) will be investigated, and sub-equation will establish by the response surface method.

With respect to the normalised ultimate strength (s_{xu}/s_Y), it may also link with the effective breadth or width of the plate concept proposed by von Kármán (1924). This concept enables approximating the complex nonlinear stress distribution in the plate element subjected to compression after buckling. This study was followed by Winter (1940) to investigate the reduction of the load-carrying capacity of a stiffened panel. It was known that out-of-plane deformations in the shape of the elastic buckling mode cause the inability of the centre of the plate to carry the compressive load. As plate deformation increases, axial stiffness of the plate may reduce so that compressive load is going to concentrate at the plate edges. The ultimate load can be captured once edge stresses experience the even exceeding yield strength of the material, and it can be expressed by effective width. This is widely adopted in the steel design codes nowadays.

In briefly, the obtained normalised ultimate strength value should be matched with the ratio (b_e/b) between original plate breadth (b), and effective breadth (or width) (b_e) can be obtained. The calculation procedure to get effective breadth is presented in the Example part.

3.1 Ultimate strength calculation results

In this section, the trend of the calculated ultimate strength results is reviewed based on four materials, i.e., S235, S275, S315 and S355. It reminds us that the "S235" represents structural steel grade with a minimum yield strength of 235 MPa. As would be expected, the ultimate strength capacity tends to decrease as the plate slenderness ratio increases smoothly for all cases. In addition, the assumed formula in Eq. (4) could be applicable to present this behaviour.

A detailed investigation of the obtained outcome will be discussed further in the following sections regarding the effect of lateral pressure, initial deflection amount and material yield strength.

3.2 Investigation on each parameter's contribution to the ultimate strength capacity

The ultimate strength capacities calculated are re-plotted based on lateral pressure and initial deflection level, as shown in Figs. 5 to 8. We reconfirmed that the ultimate strength is decreased with the increased level of initial deflections. Similarly, the existence of the lateral pressure directly contributes to decreasing the ultimate strength capacity of the plate. Similar trends were captured for all materials (S235, S275, S315 and S355). The effect of lateral pressure gradually diminished as the amount of initial plate deflection increased (slight to severe).

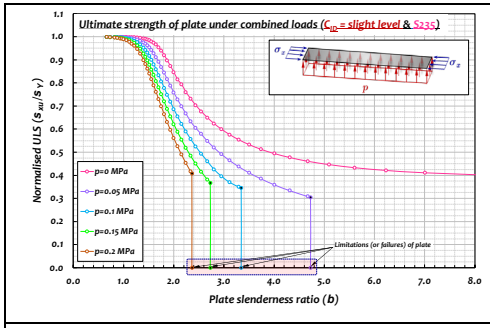	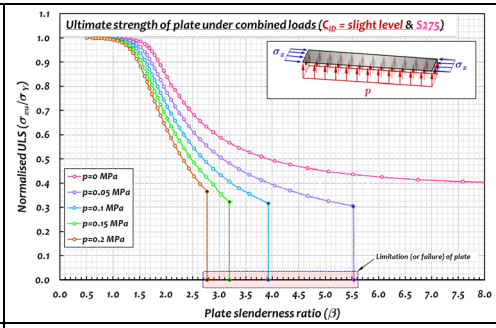	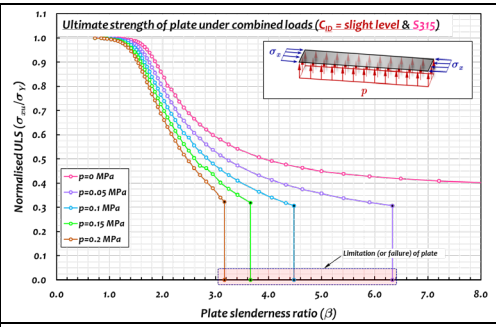	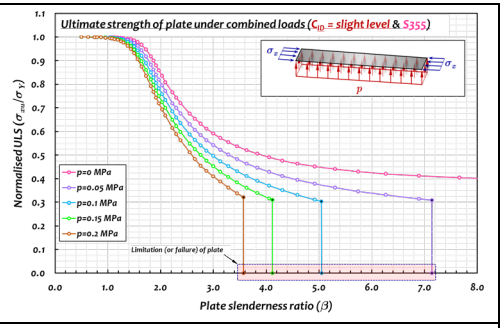
(a) slight level ($w_{opl} = 0.025b^2t$)	*(a) slight level ($w_{opl} = 0.025b^2t$)*	*(a) slight level ($w_{opl} = 0.025b^2t$)*	*(a) slight level ($w_{opl} = 0.025b^2t$)*
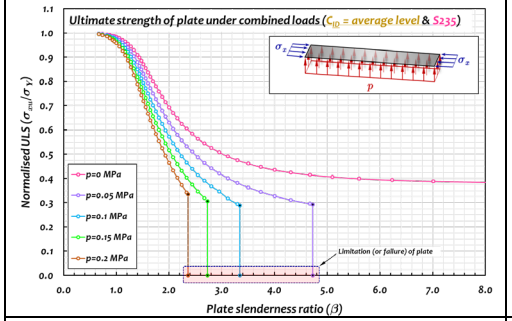	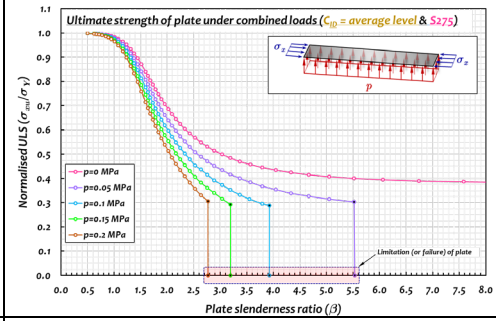	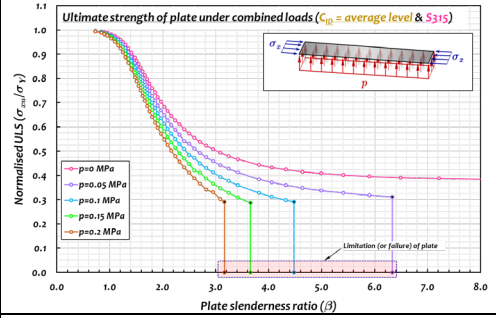	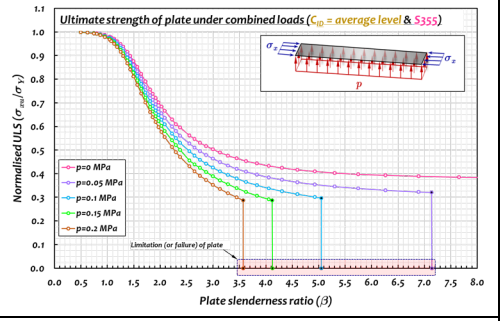
(b) average level ($w_{opl} = 0.1b^2t$)	*(b) average level ($w_{opl} = 0.1b^2t$)*	*(b) average level ($w_{opl} = 0.1b^2t$)*	*(b) average level ($w_{opl} = 0.1b^2t$)*
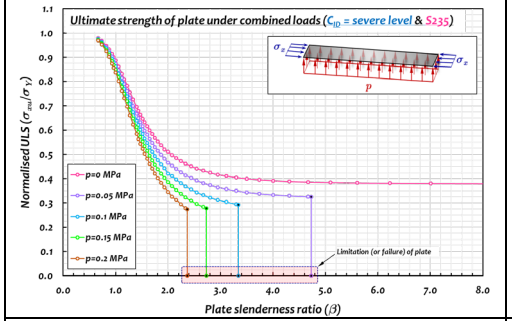	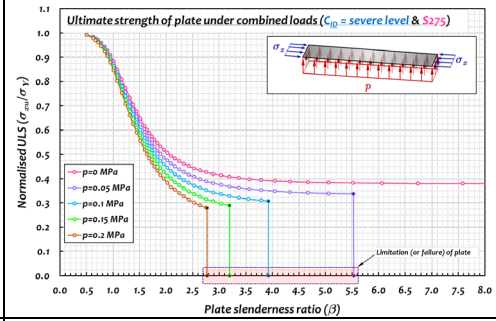	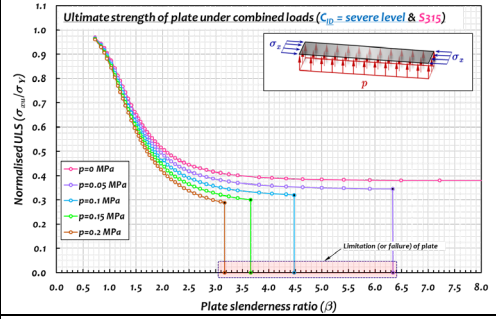	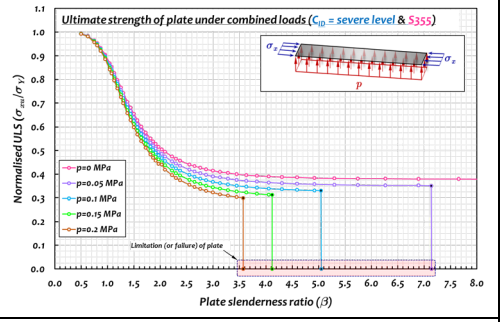
(c) severe level ($w_{opl} = 0.3b^2t$)	*(c) severe level ($w_{opl} = 0.3b^2t$)*	*(c) severe level ($w_{opl} = 0.3b^2t$)*	*(c) severe level ($w_{opl} = 0.3b^2t$)*
***Fig. 5.** Effect of initial deflection for S235 plate.*	***Fig. 6.** Effect of initial deflection for S275 plate.*	***Fig. 7.** Effect of initial deflection for S315 plate.*	***Fig. 8.** Effect of initial deflection for S355 plate.*

Statistical analysis is performed to verify this trend numerically, as shown in Fig. 9. The ultimate strength result without lateral pressure (p=0 MPa) presented on the horizontal axis, and the ULS with lateral pressure (p = 0.05, 0.1, 0.15 and 0,2 MPa) illustrated on the vertical axis. The mean and COV values were calculated as the lateral pressure changed, as illustrated in Fig. 9. A mean value of close to 1.0 represents that the ultimate strength is less affected by lateral pressure.

The ultimate strength capacity of the plate is gradually decreased as lateral pressure increases. In addition, we noted that maximum capacity also varies with the plate slenderness ratio. It means that the thinner plate has lower resistance under combined load than the thicker plate, as highlighted by the shaded box in Figs. 5 to 9. As lateral pressure increases, the maximum capacity of the plate is going to be limited, and it can be expressed by the plate slenderness ratio. It can be seen that most of the diagrams in Figs. 5 to 9 (= ULS vs. plate slenderness ratio) drops at a specific value of the plate slenderness ratio. It means that the plate is no longer withstand the applied loads, and lateral pressure may lead to the collapse of the plate. The dropped points indicate the plate slenderness ratio at ultimate limit state, which is highlighted by a shaded box. Therefore, the shaded parts do not consider for the calculation of mean and COV values. As a result, comparisons were made fairly. From here, we recognised that the limitation of the plate slenderness ratio should also be provided once we develop the empirical formula. This will be further discussed in the coming section.

We analysed the more detailed trend based on the effect of plate slenderness. As a rule of thumb, plate slenderness ratio (β) is bounded by 1.8 or 1.9 to distinguish between thin ($0 < \beta \leq 1.8$ *or* 1.9) and thick plate (1.8 *or* $1.9 < \beta$). In the present study, we assumed $\beta = 1.8$ to discriminate the thin and thick plates and calculated mean and COV based on grouped data, as shown in Fig. 10(a) to (c).

Fig. 10(a) to (c) shows the detailed statistical analysis results by showing the combination of the mean (M) and standard deviation (SD), i.e., M, M+SD, and M-SD, as a shape of the histogram. The horizontal axes show M and SD presented on the left side, and COV is also presented on the right side. From the plotted histograms, the decrement of ultimate strength due to the lateral pressure effect for thin and thick plates are investigated. For example, the mean value of 0.978 represents the 2.2% decrement of ultimate strength due to the lateral pressure effect.

The effect of lateral pressure on ultimate strength of plate increases gradually as lateral pressure increases. This is more relevant for the thin plate ($0 < \beta \leq 1.8$) than the thick plate ($1.8 < \beta$). Furthermore, in most cases, thin plates are more affected by the lateral pressure effect than thick plates. For example, 35% (orange) and 9% (green) reductions of the ultimate strength capacity are observed under 0.2 MPa lateral pressure in thin and thick plates consisting of S235 material with a slight level initial deflection.

Similarly, we investigate the effect of lateral pressure based on the level of initial deflection. As shown in Fig. 9 in the vertical direction view, we can observe that the variances between ultimate strength with and without lateral pressure are reducing from the slight level to the severe level. It means that the effect of lateral pressure is less affecting as initial plate deflection is severe. The more detailed trend can be found in the histograms in Fig. 10. Interestingly, the thin plate with severe initial deflection is less affected by lateral pressure than the thin plate with small initial deflection. In contrast, the thick plate with severe initial deflection is more affected by lateral pressure than the thick plate with small initial deflection.

In the case of material grade effect or effect of material yield strength, it is found that a higher-grade plate (= higher material yield strength) is less affected by lateral pressure. It means that ultimate strength behaviour of the high tensile steel is less sensitive than mild steel. Jiang and Zhang (2021) also indicated that stiffened plated structures with lower yield strength is more sensitive to lateral pressure, as compared with high strength steel. Their analysis was performed by NLFEM. From a physical perspective, the application of lateral pressure results in a clamped support and increases the initial stress of the plating. Thus, the collapse of the plate may be dominated by material nonlinearity (i.e., material yielding), rather than geometric nonlinearity (i.e., buckling). This is also verified by the observation that the discrepancy in Figure 2 is larger when the plate slenderness ratio is higher (more slender plate). This can be further considered with the material cost when selecting the optimised material based on safety and cost-effectiveness decisions.

For a better summary, the effect of individual parameters, i.e., material yield strength and initial deflection, on the ultimate strength capcaity of the plate is summarised again in Table 2. In this study, the plates are categorised by thin and thick conditions, but the effect of each parameter and ultimate strength behaviour varies as the plate slenderness ratio increases.

Table 2. *Summary of the individual parameter effects on the ultimate strength of the plate in association with lateral pressure.*

Condition		*Plate*	*Effect*
Initial deflection	↑	*Thin*	• *less affected by lateral pressure (than the plate with small initial deflection)*
		Thick	• *more affected by lateral pressure (than the plate with small initial deflection)*
	↓	*Thin*	• *more affected by lateral pressure (than the plate with large initial deflection)*
		Thick	• *less affected by lateral pressure (than the plate with large initial deflection)*
Material yield strength	↑	*Thin*	• *less affected by lateral pressure (than the lower grade materials)*
		Thick	• *less affected by lateral pressure (than the lower grade materials)*
	↓	*Thin*	• *more affected by lateral pressure (than the lower grade materials)*
		Thick	• *more affected by lateral pressure (than the lower grade materials)*

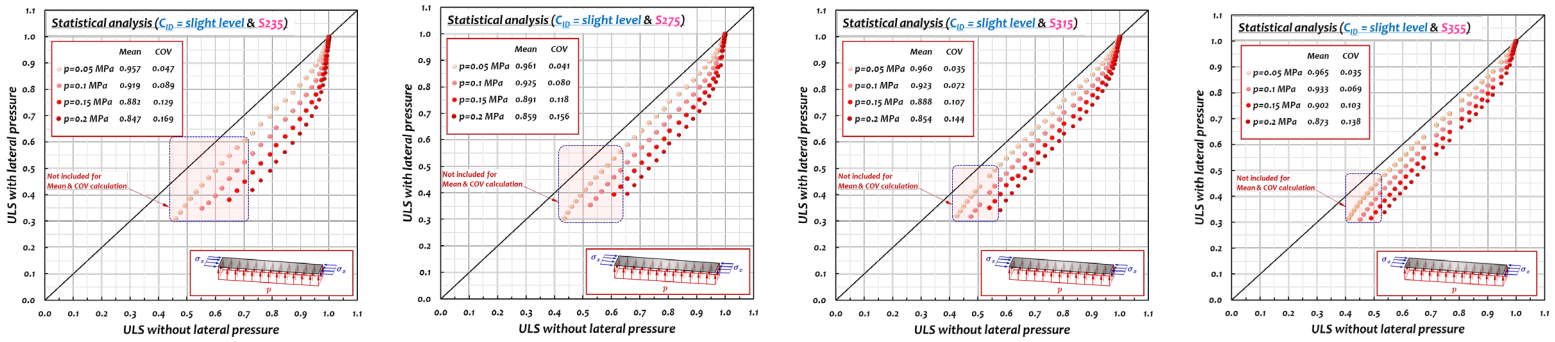

(a) slight level ($w_{opl} = 0.025b^2t$)

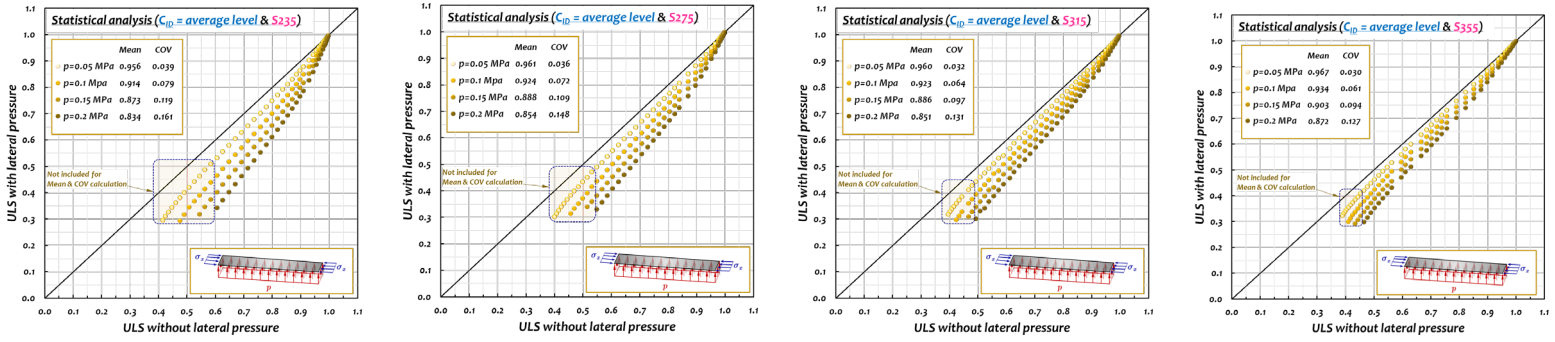

(b) average level ($w_{opl} = 0.1b^2t$)

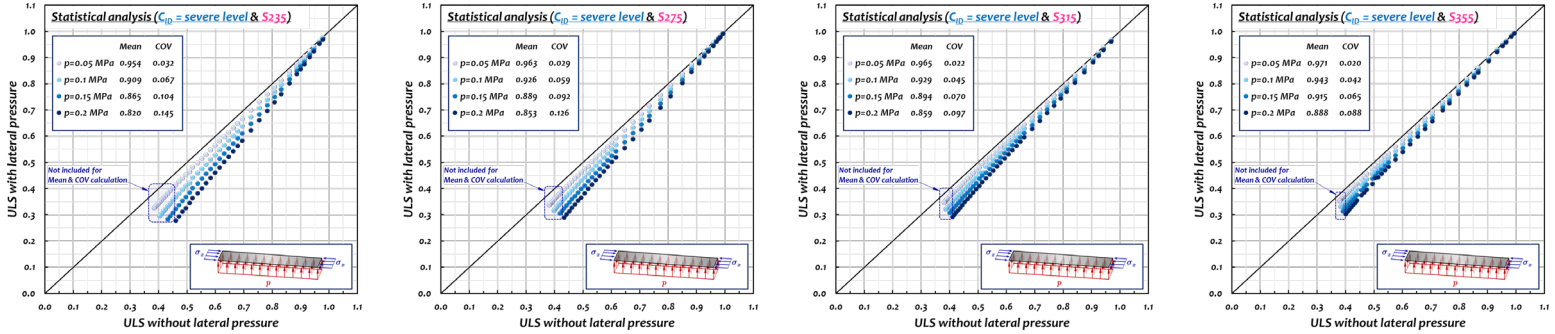

(c) severe level ($w_{opl} = 0.3b^2t$)

Fig. 9. *Statistical analysis for all plates.*

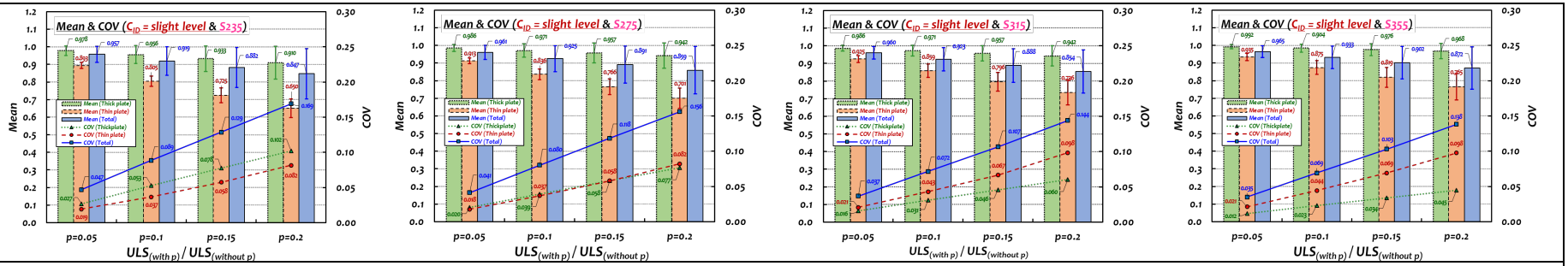

(a) slight level (w_{opl} = $0.025b^2t$)

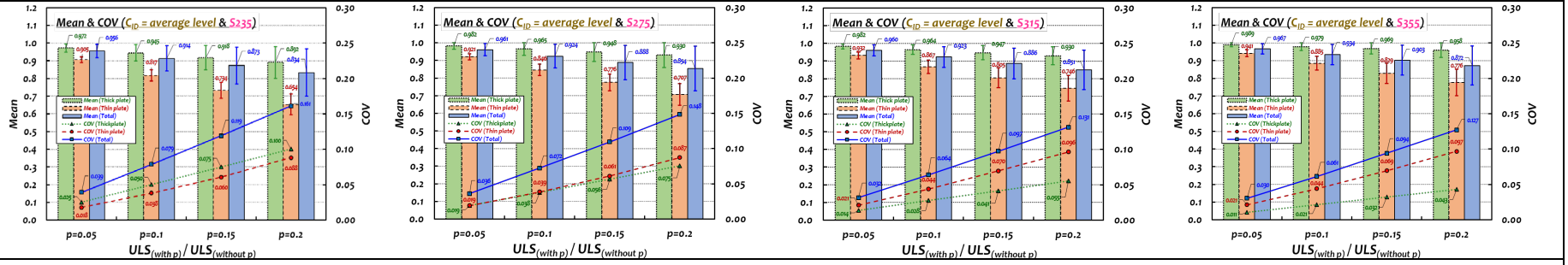

(b) average level (w_{opl} = $0.1b^2t$)

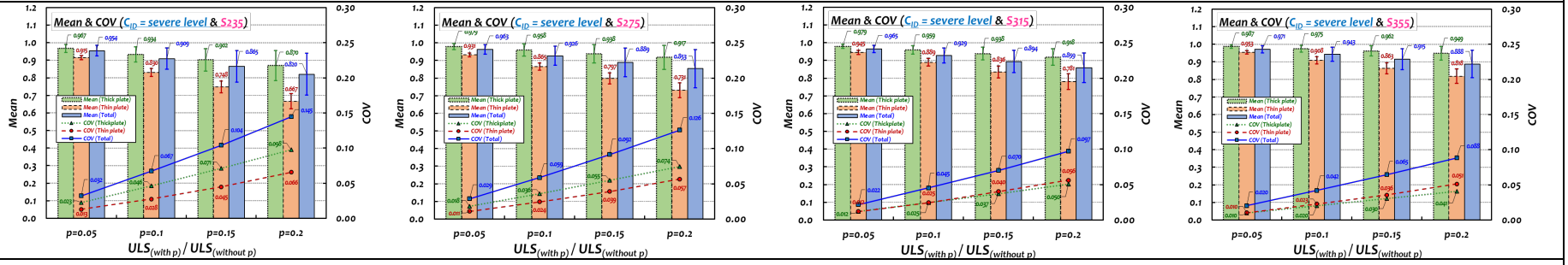

(c) severe level (w_{opl} = $0.3b^2t$)

Fig. 10. *Detailed statistical analysis for all plates based on the plate slenderness.*

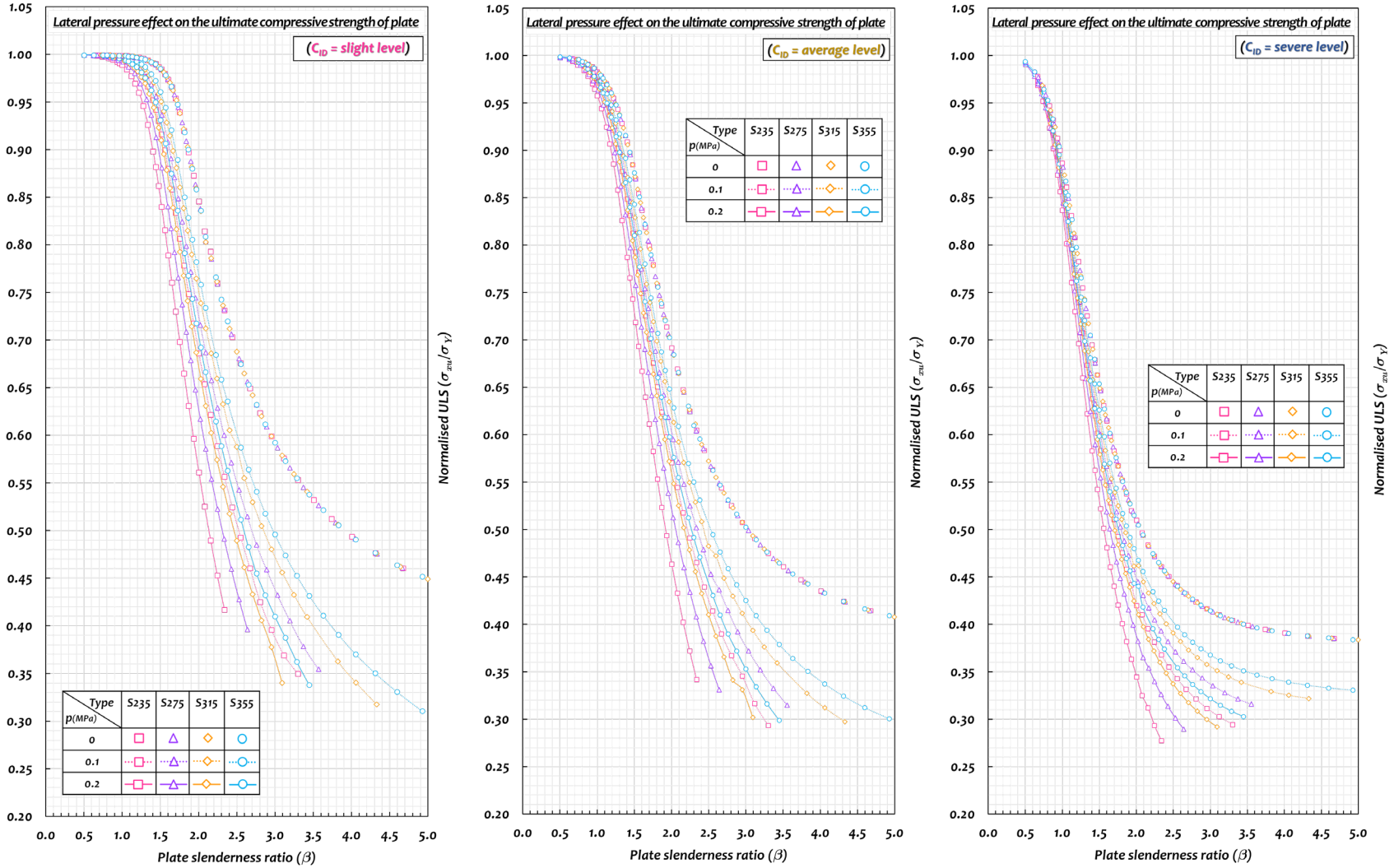

(a) slight level *(b) average level* *(c) severe level*

Fig. 11. *Lateral pressure effect on the ultimate compressive strength of plate.*

Lastly, we investigate the effect of the existence of lateral pressure on the ultimate strength of the plate, as shown in Fig. 11. As pointed out by a previous study (Kim et al., 2022; Kim et al., 2018b), the material grade does not affect the ULS behaviour of the plate without lateral pressure. It means that the ULS results by all material grades can be plotted in the same line when the plate is purely subjected to longitudinal compression, presented on the top part by various symbols in Fig. 11 (a) to (c). The ultimate strength calculation results varied as the material grade changed when the combined loads were applied, i.e., longitudinal compression and lateral pressure represented by the symbol with line. It is also observed that the ultimate strength behaviour is not always smooth, i.e., S316 with a pressure of 0.1 or 0.2 at a plate slenderness ratio of about 2.8. This seems that it is caused by the computational process when the applied lateral pressure is nearly reaching the maximum capacity of the plate. As indicated earlier in Table 2, the ultimate strength of the plate with higher graded material is less affected by lateral pressure than the lower graded material.

3.3 Mapping of the data into the empirical formula

The calculated ultimate strength capacity by ALPS/ULSAP is analysed based on structural steel grades, i.e., S235, S275, S315 and S355. As the first step of data processing, it requires that the calculated ULS results fit well with the general shape of the empirical formula in Eq. (4). One of the reliable and straightforward ways is evaluating the coefficient of determination (R^2) from the curve-fitting results.

Figure 12(a) to (d) shows the ultimate strength fitting results obtained by ALPS/ULSAP for each steel grade, i.e., S235, S275, S315 and S355. The empirical formula is also plotted based on the surface fitting curve. As would be expected, the general shape of the formula enables presenting the ultimate strength behaviour of the plate subjected to combined axial compression and lateral pressure with reliable accuracy (R^2 >0.99).

3.2.1 S235 mapping

We investigated the effect of each parameter, and the next step is the mapping of the obtained normalised ultimate limit state (ULS) to the assumed empirical formula, as mentioned

earlier. For this, we categorised input data (= ULS) based on material type, i.e., S235, S275, S315 and S355, and plotted in Fig. 12(a) to (d). Furthermore, response surface is considered as empirical formula, and five surface equations are obtained per material type based on applied lateral pressure. Relatively reliable R^2 values were achieved, and it could be practically applicable to predict the normalised ULS of the plate under combined longitudinal compression and lateral pressure.

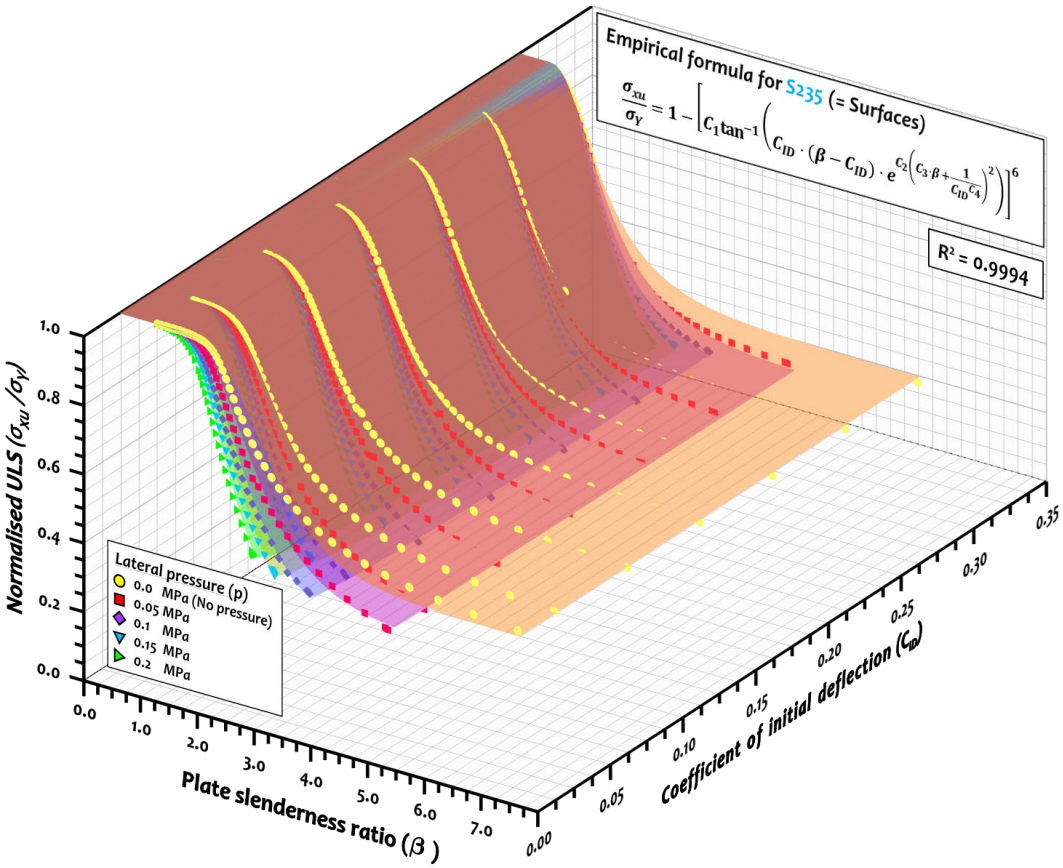

Fig. 12(a). *Ultimate strength of the plate for S235 material: ALPS/ULSAP results and empirical formula by curve-fitting method.*

Table 3(a). *Coefficient of determination (R^2) values for S235 material.*

Lateral Pressure (Mpa)	R^2	*Overall* R^2
0.00	0.9918	
0.05	0.9953	
0.10	0.9958	0.9994
0.15	0.9968	
0.20	0.9924	

Fig. 12(a) shows the fitting curves in predicting the ultimate strength of the S235 plate under combined longitudinal compression and lateral pressure. The yellow dots represent the compressive ultimate strength results of the S235 plate without lateral pressure, and the ULS tends to decrease as lateral pressure increases, which was investigated earlier. The assumed empirical formula generally shows good agreement with the results, and it can present the ULS behaviour (R^2 = 0.9994) well, as shown in Table 3(a). As investigated in Part 1 (Kim et al., 2022), the assumed empirical formula tends to slightly overestimate the ULS when the amount of initial deflection is small. When the proposed formula was developed, it was sensitive and challenging to meet all the requirements, i.e., lateral pressure amount, coefficient of initial deflection, and plate slenderness ratio. It may be available to produce better accuracy at the low value of C_{ID} by modifying the sub-coefficients (C_1 to C_4), but it may cause a similar issue at the high value of C_{ID}. Therefore, we indicate that the current formula slightly overestimates ULS when the initial deflection amount is small.

However, the empirical formula can still manage to secure a higher level of accuracy (R^2 ³ 0.9918) from the response surface equation. A similar trend has been observed in the other materials, i.e., S275, S315 and S355, as shown in Fig. 12(b) to (d). Table 3(a) to (d) also shows the accuracy of the empirical formula for each material.

3.2.2 S275 mapping

Fig. 12(b) shows the fitting curves in predicting the ultimate strength of the S275 plate under combined longitudinal compression and lateral pressure. The calculated ultimate strength results were well-fitted with the assumed empirical formula (R^2 = 0.9994). Details on the coefficient of determination can be referred to in Table 3(b). The S275 material gives an enhanced load resistance capacity (or ULS) than S235.

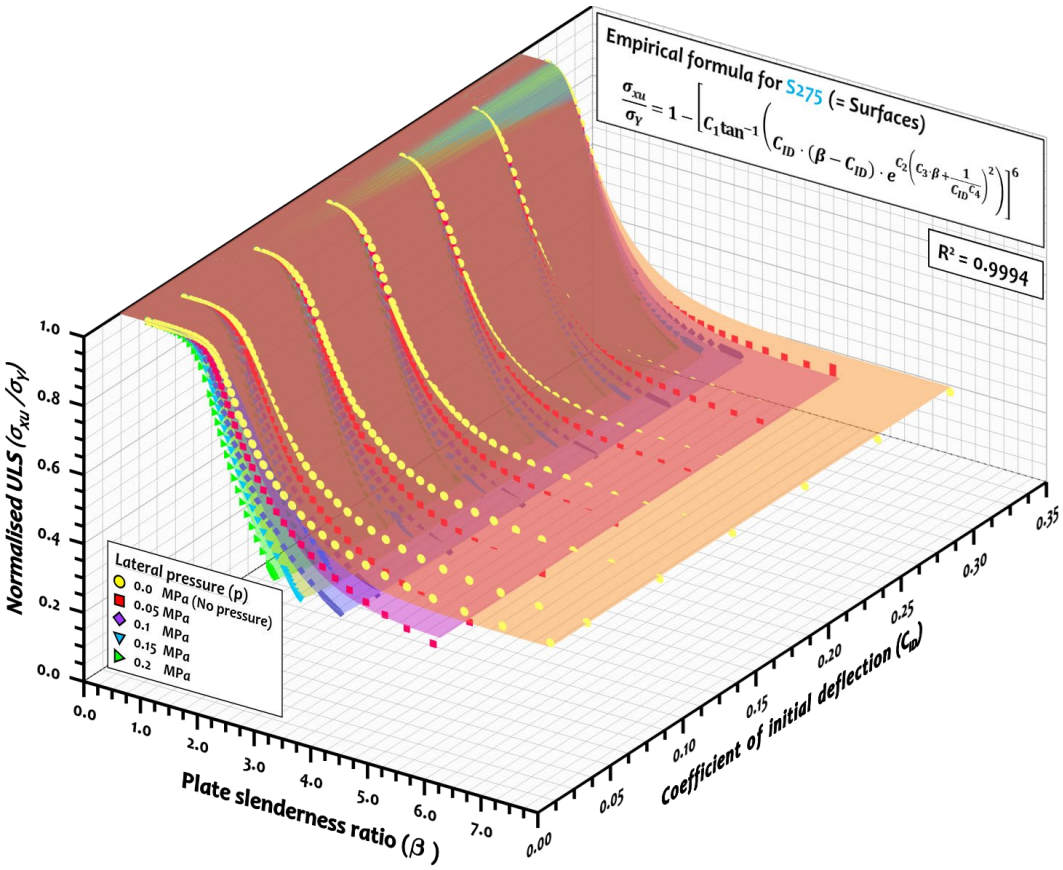

Fig. 12(b). *Ultimate strength of the plate for S275 material: ALPS/ULSAP results and empirical formula by curve-fitting method.*

Table 3(b). *Coefficient of determination (R^2) values for S275 material.*

Lateral Pressure (Mpa)	R^2	Overall R^2
0.00	0.9924	
0.05	0.9953	
0.10	0.9972	0.9994
0.15	0.9972	
0.20	0.9972	

3.2.3 S315 mapping

Fig. 12(c) shows the fitting curves in predicting the ultimate strength of the S315 plate under combined longitudinal compression and lateral pressure. The calculated ultimate strength results were well-fitted with the assumed empirical formula (R^2 = 0.9993). The S315 material gives an enhanced load resistance capacity (or ULS) than S275.

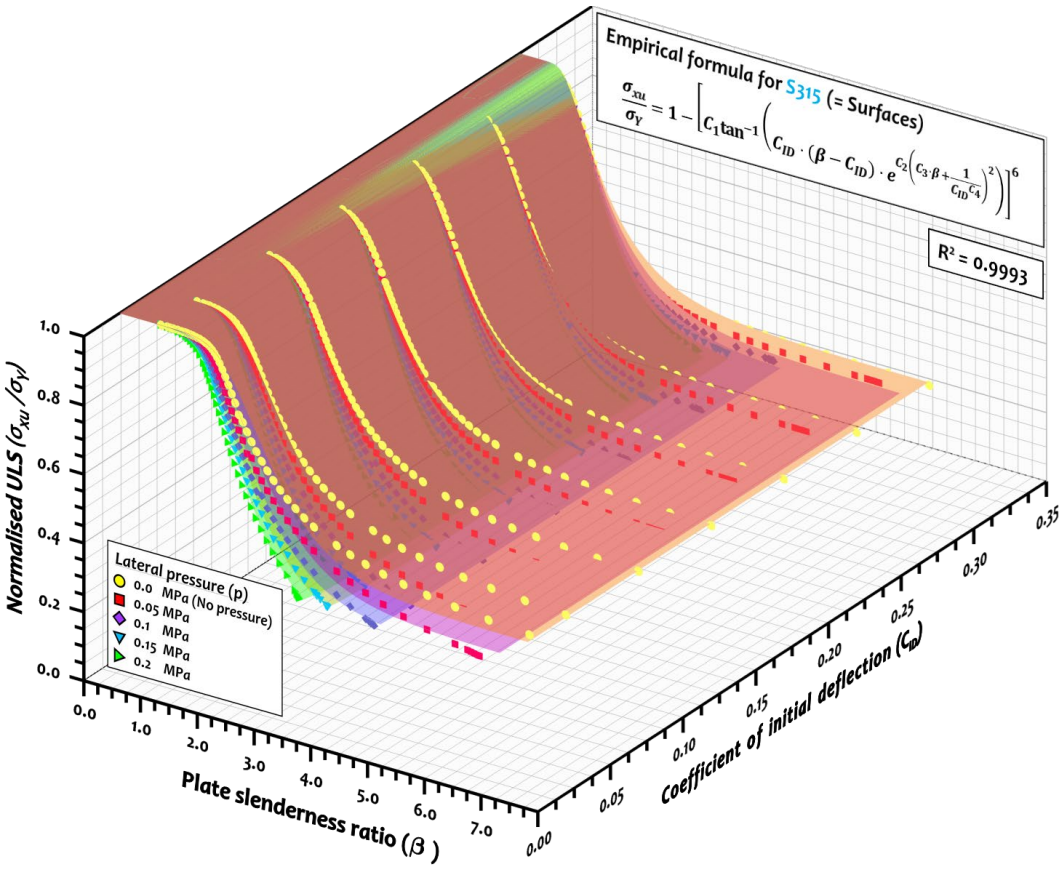

Fig. 12(c). *Ultimate strength of the plate for S315 material: ALPS/ULSAP results and empirical formula by curve-fitting method.*

Table 3(c). *Coefficient of determination (R^2) values for S315 material.*

Lateral Pressure (Mpa)	R^2	Overall R^2
0.00	0.9923	
0.05	0.9940	
0.10	0.9949	0.9993
0.15	0.9957	
0.20	0.9958	

3.2.4 S355 mapping

Fig. 12(d) shows the fitting curves in predicting the ultimate strength of the S355 plate under combined longitudinal compression and lateral pressure. The calculated ultimate strength results were well-fitted with the assumed empirical formula (R^2 = 0.9993). The S315 material gives an enhanced load resistance capacity (or ULS) than S315.

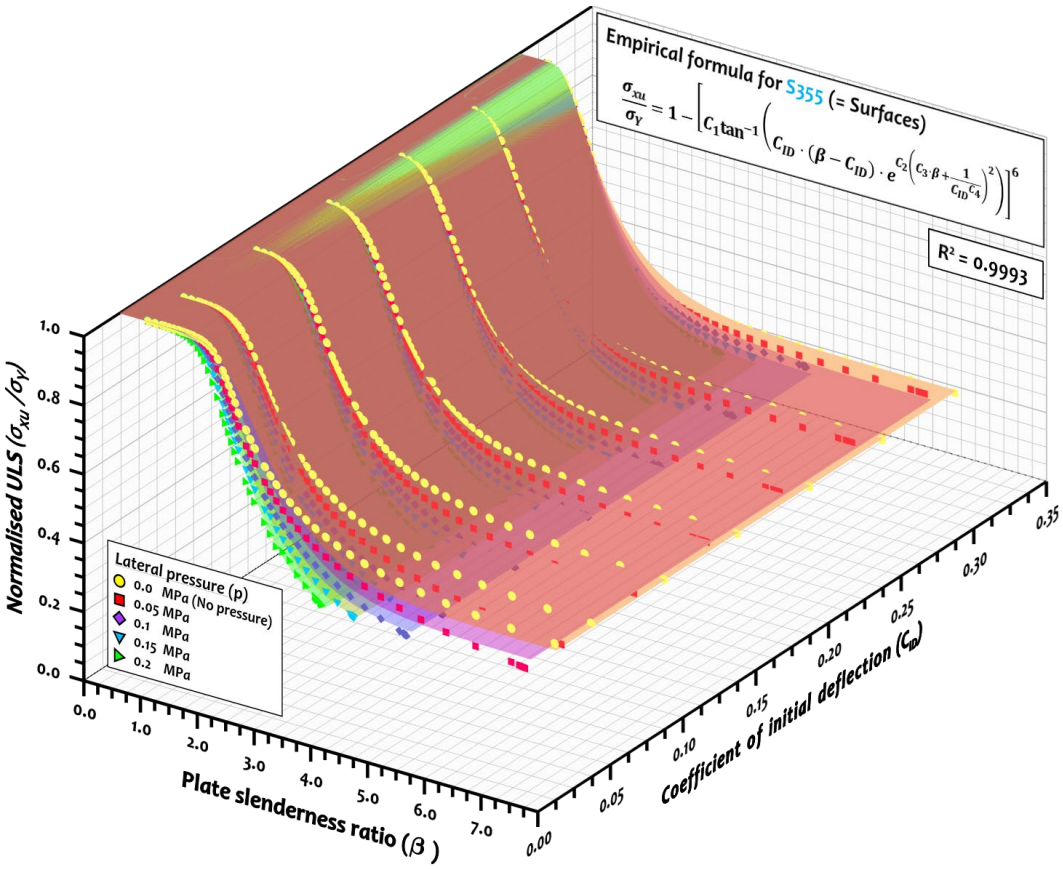

Fig. 12(d). *Ultimate strength of the plate for S355 material: ALPS/ULSAP results and empirical formula by curve-fitting method.*

Table 3(d). *Coefficient of determination (R^2) values for S355 material.*

Lateral Pressure (MPa)	R^2	Overall R^2
0.00	0.9935	
0.05	0.9947	
0.10	0.9958	0.9993
0.15	0.9963	
0.20	0.9968	

Therefore, the safety-effectiveness of the high tensile steel, i.e., structural capacity, is

confirmed. The structural designers may consider the cost-effectiveness by comparing the material cost versus structural capacity when they design the plate, i.e., outer bottom plating. Because the construction material cost varies by time and economic condition.

Until now, we confirmed that the assumed empirical formula enables structural engineers to predict the ultimate strength of the plate. However, coefficients (C_1 to C_4) have not been addressed yet, and the C_1 to C_4 are summarised in Table 4. Now, we are facing the question mark that how can we calculate the coefficients (C_1 to C_4) if the material yield strength (s_Y) is not the same as assumed cases (i.e., 235, 275, 315 and 355 MPa) or if the applied lateral pressure is a different value. To resolve this issue, this will be further discussed in section 3.2.

Table 4. *Summarised coefficients and coefficient of determinations (R^2) for all four materials.*

s_Y	p	C_1	C_2	C_3	C_4	R^2			Max. b
235	0.00	0.5853	1.5290	0.2066	0.0436	0.9918			-
235	0.05	0.5989	1.3980	0.2091	0.0732	0.9953			4.72
235	0.10	0.6061	1.3070	0.2359	0.0842	0.9958	0.9994		3.34
235	0.15	0.6133	1.2610	0.2474	0.0934	0.9966			2.73
235	0.20	0.6207	1.2420	0.2499	0.1003	0.9964			2.36
275	0.00	0.5857	1.5520	0.1968	0.0465	0.9924			-
275	0.05	0.5964	1.4470	0.1965	0.0699	0.9953			5.52
275	0.10	0.6025	1.3520	0.2195	0.0804	0.9972	0.9994		3.88
275	0.15	0.6078	1.2920	0.2371	0.0881	0.9972			3.18
275	0.20	0.6132	1.2730	0.2403	0.0941	0.9972			2.76
315	0.00	0.5867	1.5440	0.1940	0.0481	0.9923		0.9994	-
315	0.05	0.5953	1.4700	0.1904	0.0671	0.994			6.33
315	0.10	0.6000	1.3820	0.2120	0.0755	0.9949	0.9993		4.48
315	0.15	0.6040	1.3260	0.2278	0.0823	0.9957			3.65
315	0.20	0.6083	1.2810	0.2406	0.0882	0.9958			3.17
355	0.00	0.5868	1.5700	0.1842	0.0500	0.9935			-
355	0.05	0.5942	1.5060	0.1793	0.0663	0.9947			7.14
355	0.10	0.5983	1.4260	0.1977	0.0734	0.9958	0.9993		5.05
355	0.15	0.6016	1.3670	0.2144	0.0788	0.9963			4.12
355	0.20	0.6047	1.3200	0.2290	0.0834	0.9968			3.57

Note: Maximum b represents the limitation of the plate slenderness ratio to use the empirical formula, and this will be discussed in Section 3.2.

3.3 Development of sub-coefficient as a function of lateral pressure and yield strength

The determined coefficients (C_1 to C_4) are plotted based on applied lateral pressure and material yield strength, as shown in Fig. 13(a) to (d). The 3D surface fitting results, representing the Eq. (5), shows good agreement ($0.9739 \leq R^2 \leq 0.9947$) with coefficients data as shown in Table 5. Therefore, it is now available to utilise the developed empirical formula (Eq. 4) in predicting the ultimate strength of the initially deflected plate under axial compression and lateral pressure. The empirical formula consists of coefficients (C_1 to C_4), and those coefficients can be formulated again as the function of material yield strength and lateral pressure, as shown in Eq. (5).

General shape of coefficient formula ($C_{i=1to4}$)

$$C_{i=1\,to\,4} = S_1 + S_2(s_Y) + S_3(p) + S_4(p)^2 + S_5(p)^3 + S_6(p)(s_Y) \qquad (5)$$

where, sub-coefficients (S_1 to S_6) are summarised in Table 4.

Table 5. *Summarised sub-coefficients (S_1 to S_4).*

	C_1 *formula*	C_2 *formula*	C_3 *formula*	C_4 *formula*
S_1	0.5842×10^{-1}	1.375	2.629×10^{-1}	4.208×10^{-2}
S_2	6.550×10^{-6}	5.920×10^{-4}	-2.304×10^{-4}	1.731×10^{-5}
S_3	4.580×10^{-1}	-2.381	-2.684×10^{-1}	8.383×10^{-1}
S_4	-1.234	8.857×10^{-1}	6.591	-3.27
S_5	3.1	11.83	-20.77	7.62
S_6	-7.025×10^{-4}	1.295×10^{-3}	1.200×10^{-5}	-9.046×10^{-4}
Note: C_1 to C_4 can be calculated by substituting above S_1 to S_6 values into Eq. (5) or the following equation ($C_{i=1\,to\,4} = S_1 + S_2(s_Y) + S_3(p) + S_4(p)^2 + S_5(p)^3 + S_6(p)(s_Y)$).				

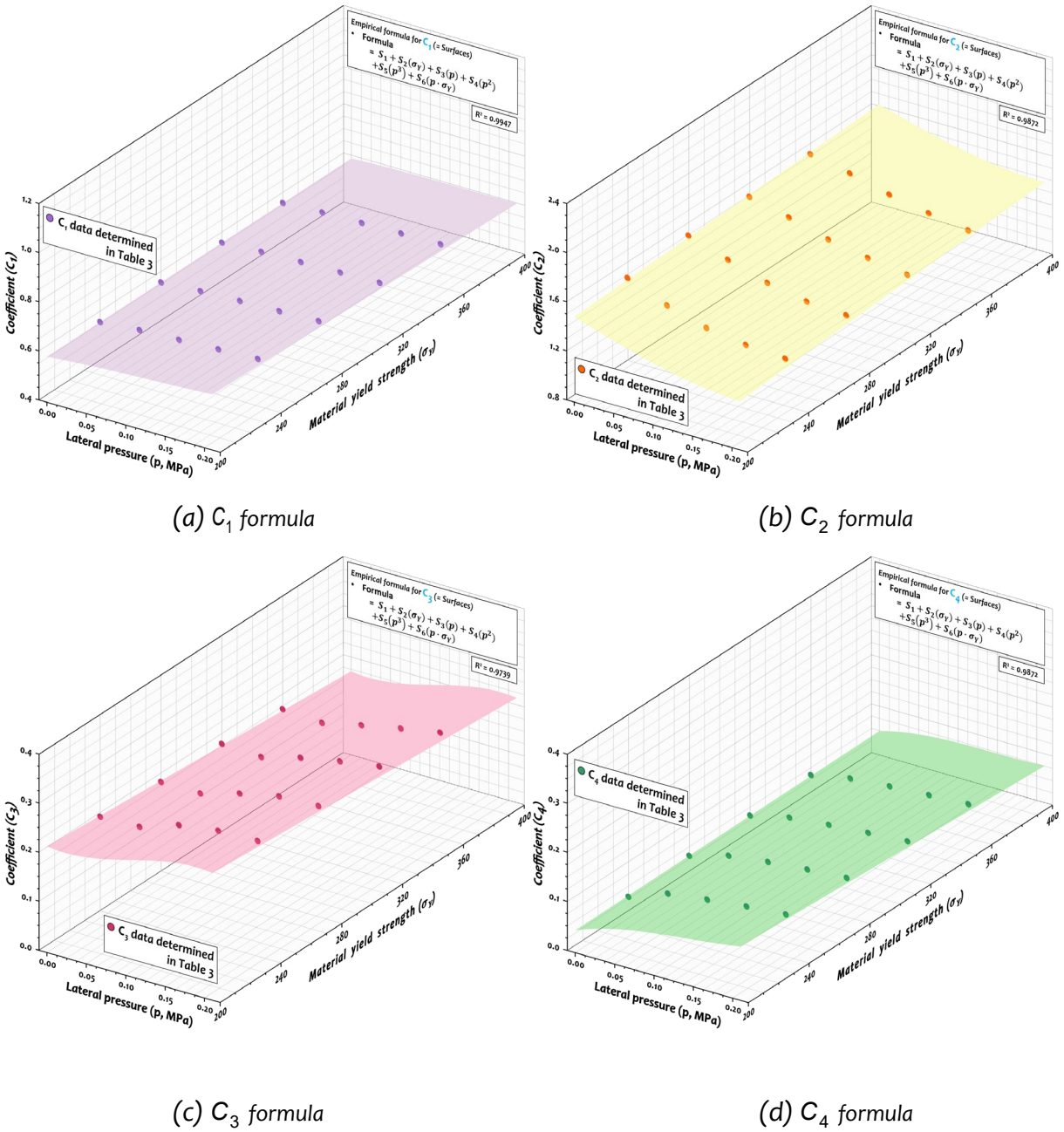

(a) C_1 *formula* *(b)* C_2 *formula*

(c) C_3 *formula* *(d)* C_4 *formula*

Fig. 13. *Formulation of the coefficients* (C_1 *to* C_4) *as a function of lateral pressure and material yield strength.*

Detailed procedure to utilise the proposed empirical formula will be discussed again in section 4. Before moving on to the next section, the range of use of the empirical formula should be clearly defined. Fig. 14 shows the example to determine the limitation of the plate slenderness ratio by highlighting boxes. Once the plate collapsed, the normalised ULS dropped to 0.0, and we conducted additional simulations by ALPS/ULSAP to find the limit value.

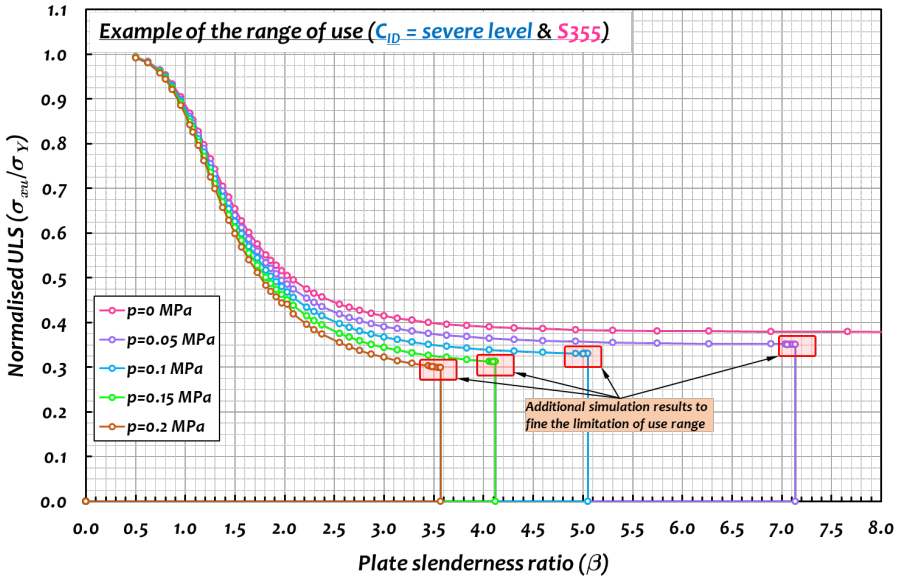

Fig. 14. *Formulation of the coefficients (C_1 to C_4) as a function of lateral pressure and material yield strength.*

By repeating this, the limitation fitting curve is proposed in Fig. 15 as a shape of a 3D response surface. From the obtained fitting curve, following Eq. (6.1) is finally obtained to limit the range of use of plate slenderness ratio. Therefore, the calculated plate slenderness ratio (b) need to be managed not to exceed b_{Limit}. If the selected b does not satisfy the limitation criteria, the material or geometric properties of the plate should be revised.

Limitation of plate slenderness ratio

$$b_{Limit} = 1.108 - 35.52(p) + 0.028(s_Y) + 321.2(p)^2 - 0.175(s_Y)(p) - 860.1(p)^3 + 0.437(s_Y)(p)^2 \quad (6.1)$$

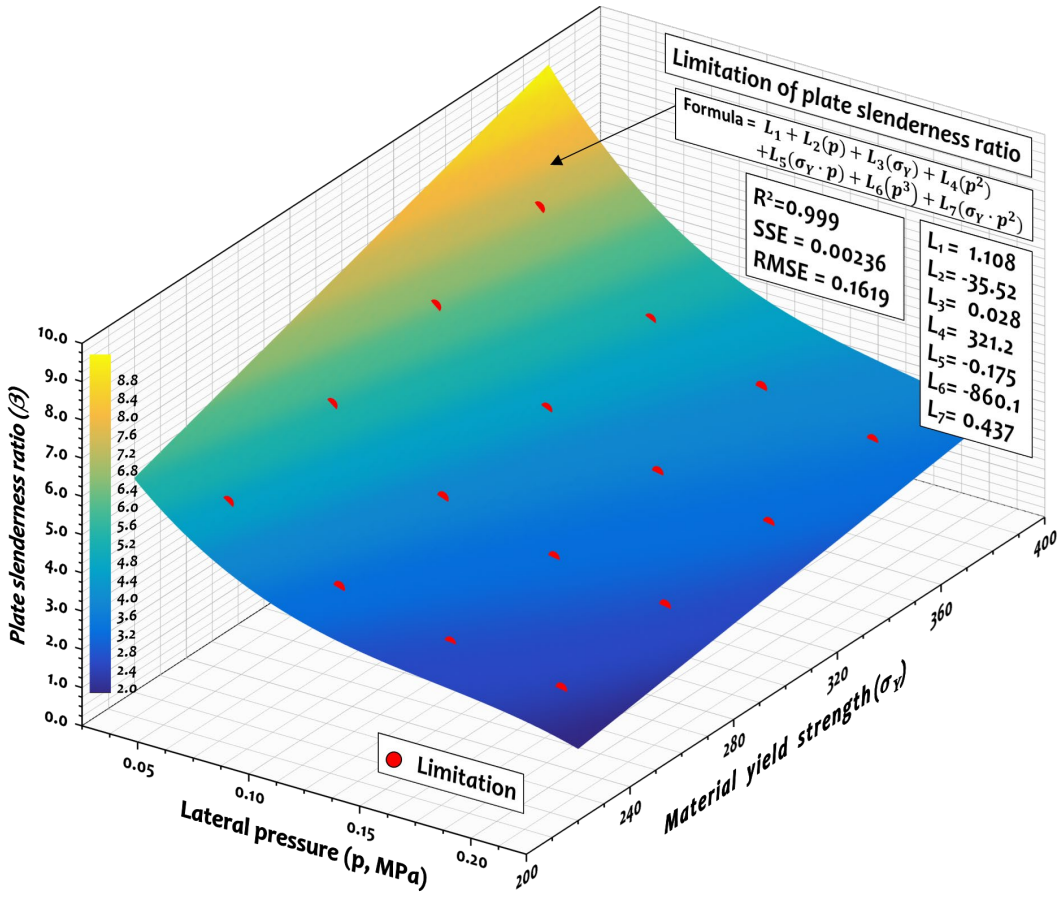

Fig. 15. *Range of use for the empirical formula developed in this study.*

By utilising the same data set shown in Fig. 15, one more meaningful formulation is obtained in Eq. (6.2) to provide the applicability range of lateral pressure. From the obtained equation, structural designers may easily predict the lateral pressure limit at the pre-FEED stage.

Limitation of lateral pressure ($R^2 = 0.9994$)

$$p_{Limit} = 0.06009 + 0.00266(s_Y) - 0.1429(b) + 3.074 \times 10^{-6}(s_Y)^2 - 0.00121(s_Y)(b) + 0.05512(b)^2 - 4.487 \times 10^{-7}(s_Y)^2(b) + 0.00014(s_Y)(b)^2 - 0.0058(b)^3 \quad (6.2)$$

4. Use of empirical formula

In the digital era, internet news and e-books are preferred over conventional newspapers and paper books. Nowadays, personalised news based on each individual's tendency is provided on smartphones rather than TV news. Users can easily find the services they want through Google, YouTube, Netflix, and others. In other words, users are no longer as patient as they used to be, preferring an immediate, easy and convenient approach. Writing journal papers and classes in schools are also expected to change soon. This means how beneficial the technology should be and how readily practical a design guide should be provided rather than just securing how good a technology is.

This section provides practical guides and tips that identify how future structural design engineers and engineering students can utilise the developed formula via tutorials in Section 4.2. We also discuss detailed procedures for using the previously developed formulas in Section 4.1.

4.1 How to use an empirical formula in predicting ultimate strength of the plate under combined longitudinal compression and lateral pressure

Prior to covering the applied example in section 4.2, the following steps may remind the readers of how to utilise the developed empirical formula for predicting the ultimate strength of the plate under combined load. There are seven essential steps introduced in Fig. 16. The other steps (1, 2, 4, 6, 7) might be simple to follow up. However, three evaluation steps are needed to evaluate the global (step 3), local strength (step 8), and use of range (= limitation of plate slenderness ratio, step 5), respectively.

As indicated in step 3, considered global strength assessment, the selected material yield strength should not be less than the calculated compressive stress. The calculated bending stress applied to the mid-ship section, i.e., at the deck, inner bottom, outer bottom, etc., can be calculated by the flexural formula ($s_{bending} = My/I$).

In step 4, we evaluate the selected plate slenderness ratio, whether it exceeds the limitation or not, before utilising the empirical formula. Once we calculate the ultimate strength of the plate, the local strength assessment can be conducted, as shown in step 8. If there are other types of empirical or design formulas, it can replace the Eq. (4) shown in Step 7.

The proposed flowchart in the present form does not include the safety assessment of the stiffened panel, but this could be easily extended for the stiffened panel. For instance, the existing empirical formulas in predicting the ultimate strength of the stiffened panel (Khedmati et al., 2016; Kim et al., 2017; Kim et al., 2019a; Kim et al., 2020; Paik and Thayamballi, 1997; Xu et al., 2018) can be utilised in steps 7 and 8, similar to the safety assessment of the unstiffened plate. In addition, column slenderness ratio ($\lambda = (a/pr)\sqrt{s_{Yeq.}/E}$) may be required together with plate slenderness ratio to define the limitation and calculate the ultimate strength.

For the last step, we can complete the design of the plate based on the global and local safety assessment of the plate. If the condition assessment of the plate is the only target for readers, Step 4 to Step 7 will be good enough.

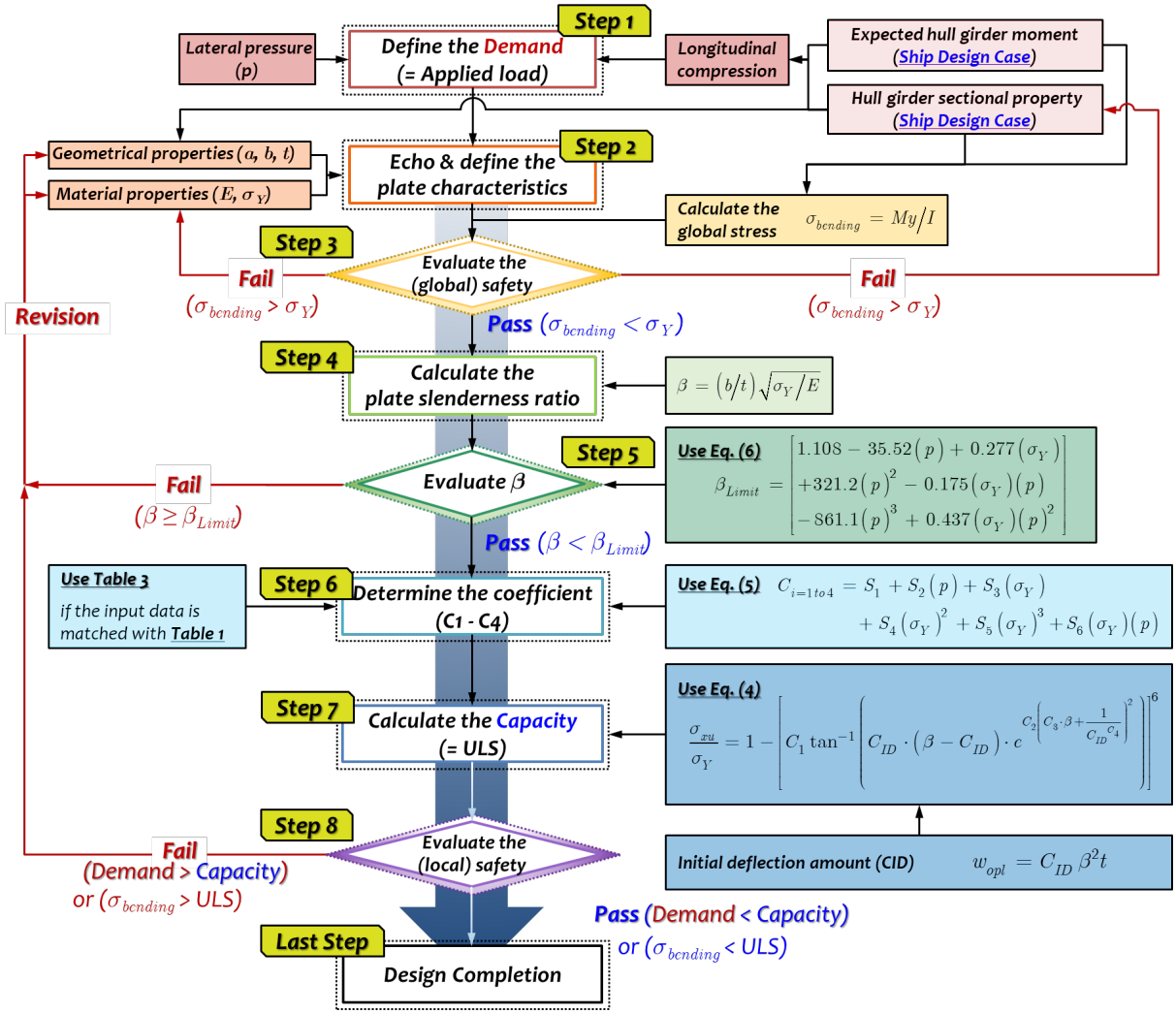

Fig. 16. *Use of the empirical formula for the design of the plate.*

4.2 Tutorial (= applied example) for readers

The applied example may help potential readers, including structural engineers, designers, academic lecturers, students, and many others. The three examples will be provided to predict the plate's ultimate strength under combined lateral pressure and longitudinal compression.

4.2.1 Example No. 1 (Simple version: Prediction of the plate's ultimate strength capacity only)

Let us assume that a plate ($a \times b \times t = 5000mm \times 1000mm \times 20mm$) consists of mild steel 24kgf (= yield strength = $24 \times 9.81 = 235.44 \; ; \; 235MPa$) is subjected to longitudinal compression and lateral pressure (p = 0.15 MPa). Determine the ultimate strength of the plate (Note: Elastic modulus can be assumed as 205.8 GPa & Apply the average level initial deflection).

(Solution)

1. [Input data echo]

$$a = 5,000mm \; ; \; b = 1,000mm \; ; \; t = 20mm \; ; \; s_Y = 235MPa \; ; \; E = 205,800MPa \; ; \; p = 0.15MPa .$$

2. [Recall – Step 4] Calculate the plate slenderness ratio

$$b = \frac{b}{t}\sqrt{\frac{s_Y}{E}} = \frac{1000}{20}\sqrt{\frac{235}{205800}} = 1.689589$$

$$\therefore \; \underline{b \; ; \; 1.6896}$$

3. [Recall – Step 5] Check the limitation of plate slenderness ratio

$$b_{Limit} = \left[1.108 - 35.52(p) + 0.028(s_Y) + 321.2(p)^2 - 0.175(s_Y)(p) - 860.1(p)^3 + 0.437(s_Y)(p)^2 \right]$$

$$= \left[1.108 - 35.52(0.15) + 0.028(235) + 321.2(0.15)^2 - 0.175(235)(0.15) - 860.1(0.15)^3 + 0.437(235)(0.15)^2 \right]$$

$$; \; 2.8261$$

$$b(= 1.6896) < b_{Limit}(= 2.8261) \qquad \therefore \; \underline{Satisfied!}$$

4. [Recall – Step 6] Determine the coefficients (C_1 to C_4)

In this case, yield strength (= 235 MPa) and lateral pressure (= 0.15 MPa) are selected scenarios shown in Table 1. Therefore, the following coefficients can be utilised as presented in Table 3.

$C_1 = 0.6133;\quad C_2 = 1.261;\quad C_3 = 0.2474;\quad C_4 = 0.0934.$

Note: The coefficients should be calculated if the yield strength and lateral pressure do not match with the selected scenarios in this study.

5. [Recall – Step 7] Calculate the ultimate strength

$$\frac{s_{xu}}{s_Y} = 1 - \left\{C_1 \tan^{-1}\left[C_{ID} \times (b - C_{ID}) \times e^{C_2 \left(C_3 \times b + \frac{1}{C_{ID}^{C_4}}\right)^2}\right]\right\}^6$$

$$= 1 - \left\{0.6133 \tan^{-1}\left[0.1(1.6896 - 0.1) \times e^{1.261\left(0.2474(1.6896) + \frac{1}{0.1^{0.0934}}\right)^2}\right]\right\}^6$$

$$; \quad 0.5066$$

$$\therefore s_{xu} = 0.5066 \times 235 MPa = \underline{119 MPa}$$

From the obtained value (= 0.5066) and original plate breadth (b = 1000mm) information, we can also predict the effective breadth/width of the plate as follows.

$$\frac{s_{xu}}{s_Y} = \frac{b_e}{b}; \quad 0.5066$$

$$\therefore b_e = 0.5066 \times 1,000 mm = \underline{506.6 mm}$$

4.2.2 Example No. 2 (Detailed version: Safety assessment of the plate)

Example No. 1 covered a simplified tutorial question to predict the ultimate strength of the initially deflected plate under combined longitudinal compression and lateral pressure. Here, a more concise example of predicting the ultimate strength and assessing the safety will be provided, including the global and local strength assessment and its safety.

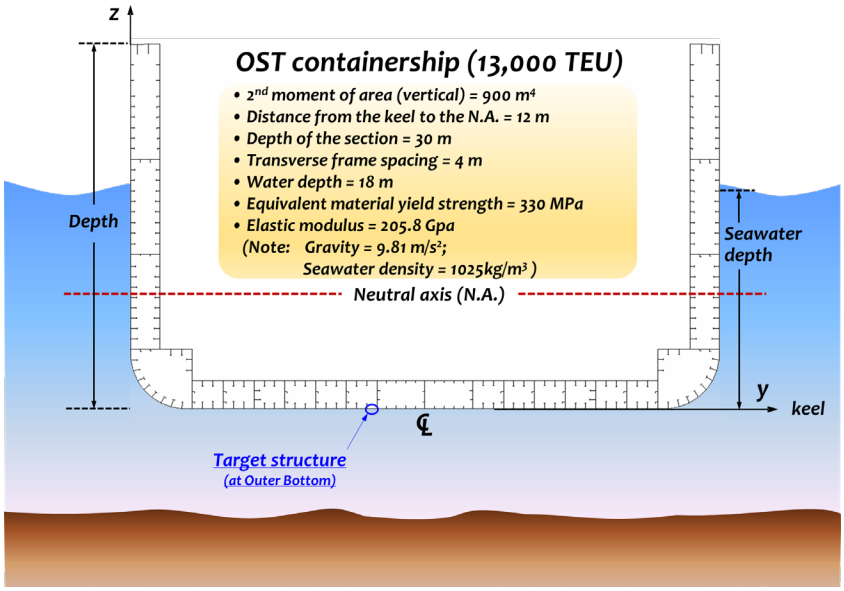

Fig. 17. *Example of the container ship (Note: The given values are assumed).*

Let us assume a container ship designed to withstand the extreme hogging moment of 16,000 MNm. The sectional properties of the mid-ship section are summarised in Fig. 17. Assess the safety of the outer bottom plate ($a \times b \times t = 4000mm \times 800mm \times 20mm$), which is initially deflected (= $w_{opl} = 0.2b^2t$). If the plate does not satisfy the safety requirement, redesign the plate by increasing the thickness of the plate, i.e. 1 mm per trial.

(Solution)

1. [Input data echo]

- *Plate data*

  $a = 4,000mm;\ b = 800mm;\ t = 20mm;\ s_Y = 330MPa;\ E = 205,800MPa;\ C_{ID} = 0.2.$

- *Hull section data (Necessary items only)*

  $I_{xx(vertical)} = 900m^4;\ N.A. = 12m.$

- *Environmental data & Applied load*

  $r_{sw} = 1,025\ kg/m^3;\ g = 9.81\ m/s^2;\ h = 18m\ (water\ depth);\ M = 16,000MNm.$

2. [Recall – Step 2] Define the demand (D)

- *Lateral pressure*

$$p = r_{sw} \times g \times h = 1025 kg/m^3 \cdot 9.81 m/s^2 \cdot 18m = 0.180995 MPa$$

$$\therefore p ; \underline{0.181 MPa}$$

- *Longitudinal compression caused by hull girder bending moment*

$$s_{bending} = \frac{My}{I_{xx}} = \frac{M(N.A.)}{I_{xx}} = \frac{16,000 MNm(12m)}{900 m^4} = 213.3333 MPa$$

$$\therefore s_{bending} ; \underline{213.3 MPa}$$

3. [Recall – Step 3] Evaluate the global safety

$s_{bending} (= 213.3 MPa) < s_Y (= 330 MPa)$ $\therefore$ *Safe*!

4. [Recall – Step 4] Calculate the plate slenderness ratio

$$b = \frac{b}{t}\sqrt{\frac{s_Y}{E}} = \frac{800}{20}\sqrt{\frac{330}{205800}} = 1.601748$$

$$\therefore b ; \underline{1.6017}$$

5. [Recall – Step 5] Check the limitation of plate slenderness ratio

$$b_{Limit} = \begin{bmatrix} 1.108 - 35.52(p) + 0.028(s_Y) + 321.2(p)^2 - 0.175(s_Y)(p) - 860.1(p)^3 \\ + 0.437(s_Y)(p)^2 \end{bmatrix}$$

$$= \begin{bmatrix} 1.108 - 35.52(0.181) + 0.028(330) + 321.2(0.181)^2 - 0.175(330)(0.181) - 860.1(0.181)^3 \\ + 0.437(330)(0.181)^2 \end{bmatrix}$$

$$; 3.6138$$

$b (= 1.6017) < b_{Limit} (= 3.6138)$ *Satisfied*!

6. [Recall – Step 6] Determine the coefficients (C_1 to C_4)

- ***Coefficient*** C_1

$$C_1 = S_1 + S_2(s_Y) + S_3(p) + S_4(p)^2 + S_5(p)^3 + S_6(p)(s_Y)$$

$$= \begin{bmatrix} 0.5842 + 0.00000655(330) + 0.458(0.181) - 1.234(0.181)^2 \\ + 3.1(0.181)^3 - 0.0007025(0.181)(330) \end{bmatrix} = 0.60524298$$

$\therefore C_1$; <u>0.6052</u>

- ***Coefficient*** C_2

$$C_2 = S_1 + S_2(s_Y) + S_3(p) + S_4(p)^2 + S_5(p)^3 + S_6(p)(s_Y)$$

$$= \begin{bmatrix} 1.375 + 0.000592(330) - 2.381(0.181) + 0.8857(0.181)^2 \\ + 11.83(0.181)^3 + 0.001295(0.181)(330) \end{bmatrix} = 1.3159146$$

$\therefore C_2$; <u>1.3159</u>

- ***Coefficient*** C_3

$$C_3 = S_1 + S_2(s_Y) + S_3(p) + S_4(p)^2 + S_5(p)^3 + S_6(p)(s_Y)$$

$$= \begin{bmatrix} 0.2629 - 0.00023(330) - 0.2684(0.181) + 6.591(0.181)^2 \\ - 20.77(0.181)^3 + 0.000012(0.181)(330) \end{bmatrix} = 0.231771$$

$\therefore C_3$; <u>0.2318</u>

- ***Coefficient*** C_4

$$C_4 = S_1 + S_2(s_Y) + S_3(p) + S_4(p)^2 + S_5(p)^3 + S_6(p)(s_Y)$$

$$= \begin{bmatrix} 0.04208 + 0.00001731(330) + 0.8383(0.181) - 3.27(0.181)^2 \\ + 7.62(0.181)^3 - 0.0009046(0.181)(330) \end{bmatrix} = 0.083548998$$

$\therefore C_4$; <u>0.0835</u>

7. [Recall – Step 7] Calculate the ultimate strength

$$\frac{\sigma_{xu}}{\sigma_Y} = 1 - \left\{ C_1 \tan^{-1}\left(C_{ID} \times (b - C_{ID}) \times e^{C_2 \left(C_3 \times b + \frac{1}{C_{ID}^{C_4}} \right)^2} \right) \right\}^6$$

$$= 1 - \left\{ 0.6052 \tan^{-1}\left(0.2 (1.6017 - 0.2) \times e^{1.3159 \left(0.2318 (1.6017) + \frac{1}{0.2^{0.0835}} \right)^2} \right) \right\}^6$$

$$; \quad 0.6323$$

$$\sigma_{xu} = 0.6323 \times 330 MPa = \underline{208.7 MPa}$$

From the obtained value (= 0.6323) and original plate breadth (b = 800 mm) information, we can also predict the effective breadth/width of the plate as follows.

$$\frac{\sigma_{xu}}{\sigma_Y} = \frac{b_e}{b} \; ; \quad 0.6323$$

$$\therefore \; b_e = 0.6323 \times 800 mm = \underline{505.8 mm}$$

8. [Recall – Step 8] Evaluate the local safety

$$Demand \left(\sigma_{bending} (= 213.3 MPa) \right) > Capacity \left(\sigma_{xu} (= 208.7 MPa) \right)$$

$$or \qquad Safety\ Factor = \frac{Capacity}{Demand} = 0.978 < 1.0$$

$$\therefore \; \underline{Unsafe}!$$

We are aware that the calculated safety factor (= structural adequacy or the capacity-demand ratio) is less than 1.0, which means that the designed plate is not satisfying the safety requirement. Therefore, plate thickness updating is needed from the given 20mm to 21mm to get a revised plate slenderness ratio (Step 4), as follows.

$$\beta = \frac{b}{t}\sqrt{\frac{\sigma_Y}{E}} = \frac{800}{21}\sqrt{\frac{330}{205800}} = 1.525475$$

$$\therefore \; \beta \; ; \; \underline{1.5255}$$

The ultimate strength recalculation is also followed.

$$\frac{\sigma_{xu}}{\sigma_Y} = 1 - \left\{0.6052 \tan^{-1}\left(\left\{0.2\left(1.5255 - 0.2\right)\right\}^{1.3159}\left\{0.2318\left(1.5255\right) + \frac{1}{0.2^{0.0835}}\right\}^{2}\right)\right\}^{6}$$

$$; \quad 0.6662$$

$$\sigma_{xu} = 0.6662 \times 330MPa = \underline{219.8MPa}$$

The local safety can be reassessed as follows, and the design can be completed.

$$Demand \left(\sigma_{bending} (= 213.3MPa)\right) > Capacity \left(\sigma_{xu} (= 219.8MPa)\right)$$

$$or \qquad Safety\ Factor = \frac{Capacity}{Demand} = 1.03 > 1.0$$

$$\therefore \ \underline{Safe}!$$

4.2.3 Discussion

In section 4, a concise flowchart type user guide is provided. Two practical examples are also given and solved to understand better how to utilise the proposed empirical formula. In addition, a detailed procedure to assess the global and local safety of the ship structure is summarised. The proposed user guide and empirical formula may apply to the deck plating in ship structures.

The formula proposed in this study is developed by assuming the plate boundary condition as simply supported. It should be stressed that the unstiffened panel (= plate) and stiffened panel in the outer bottom is assumed as the clamped condition. Therefore, the calculated ultimate strength in Example 2 underate the structural capacity by allowing rotational degree freedom at the edge of the plate. However, this can be considered a pessimistic design concept for the plate, enabling it to secure the additional safety margin.

Regarding the initial deflection of the plate, the buckling shape, widely applied in the field of structural engineering, is assumed. However, it should be emphasised that the three initial deflection levels, i.e., slight ($w_{opl} = 0.025b^2t$), average ($w_{opl} = 0.1b^2t$), and severe ($w_{opl} = 0.3b^2t$) proposed by Smith et al. (1988) assumed a hungry horse mode shape. Regarding the buckling mode shape and amplitude, the limitation of the assumed buckling mode shape and maximum deflection are documented in Part 1 (Kim et al., 2022). In brief, Smith's equation provides the measured maximum initial deflection based on hungry horse mode. The sinusoidal curve type (= buckling mode shape) initial deflection with the amplitude of Smith's formula is not a realistic assumption, and it underrates the ultimate strength capacity. However, the proposed empirical

formula and assumed buckling mode shape in this study can consider the wide range of the initial deflection coefficient (C_{1D}) so that it enables us to consider the measured or averaged initial deflection amount along with the plate length. In addition, the effect of initial deflection shape is less affecting the ultimate strength capacity when the lateral pressure is applied to the plate.

In the future, the clamped condition or partially rotation-constrained condition (Kee Paik et al., 2011) may be considered to develop the empirical formula using the general shape in Eq. (1)(Kim et al., 2018b) or Eq. (4)(Kim et al., 2022). In addition, data processing may be possible through techniques that have recently been in the spotlight, such as machine learning or neural network-based deep learning (Oh et al., 2020; Wong and Kim, 2018).

5. Conclusion

5.1 Obtained Outcomes

This study aimed to provide an empirical formula in predicting the ultimate strength of the initially deflected plate under combined lateral pressure and longitudinal compression. The obtained outcomes are summarised as follows.

- *A useful empirical formula is proposed, including a specific limitation of the plate slenderness ratio, to predict the ultimate strength capacity of the initially deflected plate under combined longitudinal compression and lateral pressure (See Fig. 16).*
- *The obtained outcome was well-fitted with ALPS/ULSAP semi-analytical solutions with an average R^2 value of 0.9994 (See Table 4).*
- *The effect of various yield stress and lateral pressure on the ultimate compressive strength of the initially deflected plate is investigated and summarised (See section 3.2).*
- *A detailed procedure to utilise the obtained empirical formula is documented (See section 4.1), including the valuable tutorials used for a lecture or design guide (See section 4.2).*

5.2 Limitation & Required further study

Modern containerships have very thick plates on the hatch corner, the main deck, and the upper part of the inner hull and side shell. However, these plates are made of high tensile steel with a yield limit of 415, 455, and the geometry is different from the one considered in this study. The stiffener spacing, the span is double, etc. Moreover, even using the NLFEM method, it is challenging to validate the ULS analyses for such very thick stiffened panels used in the construction of container ships. It seems that the ALPS/ULSAP method has less accuracy for thick plates, which is above 40 mm.

Therefore, further study can be conducted by considering thick plates, higher-grade materials, different boundary conditions, dynamic pressure effect, etc. In addition, other types of data processing techniques, i.e., artificial intelligence, including machine learning and deep learning, can also be applied.

Acknowledgement

This work was supported by the New Faculty Startup Fund from Seoul National University and the framework of international cooperation program managed by the National Research Foundation of Korea (NRF-2022K2A9A2A23000266).

References

Uncategorized References

AISC, 1961. Specification for the design, fabrication and erection of structural steel for buildings. American Institute of Steel Construction, Chicago, IL, USA.
ALPS/ULSAP, 2016. A computer program for ultimate limit state assessment of plates and stiffened panels. Advanced Technology Center, DRS C3 Systems, Parsippany, NJ, USA.
Benson, S., Downes, J., Dow, R.S., 2015. Overall buckling of lightweight stiffened panels using an adapted orthotropic plate method. Engineering Structures 85, 107-117.
Brubak, L., Andersen, H., Hellesland, J., 2013. Ultimate strength prediction by semi-analytical analysis of stiffened plates with various boundary conditions. Thin-Walled Structures 62, 28-36.
BS153, 1966. Steel Girder Bridges, Part 4, Design and Construction, in: Insitution, B.S. (Ed.), London, UK.
BS499, 1961. The use of structural steel in building and Addendum, in: Insitution, B.S. (Ed.), London, UK.
Carlsen, C.A., 1977. Simplified collapse analysis of stiffened plates. Norwegian Maritime Research 5 (4), 20-36.
Chen, Q., Hanson, R., Grondin, G., 2004. Interactive buckling testing of stiffened steel plate panels, SSC-433, Marine Structure Committee, Washington, USA.
Chen, Y., 2003. Ultimate strength analysis of stiffened panels using a beam-column method. Virginia Polytechnic Institute and State University, Blacksburg, VA, USA.
Chilver, A.H., 1953. The maximum strength of the Thin–walled Channel Strut. Civil Engineering and Public Works Review 48, 1143-1146.
Cox, H.L., 1933. The Buckling of Thin Plates in Compression. R. & M. No. 1554. British Aeronautical Research Committee (ARC).
Cui, W., Mansour, A.E., 1998. Effects of welding distortions and residual stresses on the ultimate strength of long rectangular plates under uniaxial compression. Marine Structures 11 (6), 251-269.
Dwight, J.B., Moxham, K.E., 1969. Welded Steel Plates in Compression. The Structural Engineering 47 (2), 49-66.
Faulkner, D., 1975. A Review of Effective Plating for Use in the Analysis of Stiffened Plating in Bending and Compression. Journal of Ship research 19 (1), 1-17.
Faulkner, D., 1977. Compression Tests on Welded Eccentrically Stiffened Plate Panels Crosby Lockwood Publishers, London, UK.
Frankland, J.M., 1940. The strength of ship plating under edge compression. US Expermental Model Basin Progress Report 469.
Fujikubo, M., Harada, M., Yao, T., Reza Khedmati, M., Yanagihara, D., 2005. Estimation of ultimate strength of continuous stiffened panel under combined transverse thrust and lateral pressure Part 2: Continuous stiffened panel. Marine Structures 18 (5), 411-427.
Georgiadis, D.G., Samuelides, M.S., Li, S., Kim, D.K., Benson, S., 2021. Influence of stochastic geometric imperfection on the ultimate strength of stiffened panel in compression, The 8th International Conference on Marine Structures (MARSTRUCT 2021), 7-9 June, Trondheim, Norway.
Gerard, G., 1957. Handbook of structural stability part IV: failure of plates and composite elements. New York University, New York, Washington DC, USA.
Gordo, J.M., Soares, C.G., 2008. Compressive tests on short continuous panels. Marine Structures 21 (2), 113-137.
Guedes Soares, C., 1988. Design equation for the compressive strength of unstiffened plate elements with initial imperfections. Journal of Constructional Steel Research 9 (4), 287-310.
Hughes, O.F., 1983. Ship structural design: a rationally-based, computer-aided, optimization approach. Wiley-Interscience, New York, NY, USA.
Hughes, O.F., Paik, J.K., 2010. Ship structural analysis and design. Published by: The Society of Naval Architects and Marine Engineers, SNAMNE, New Jersey, ISBN: 978-0-939773-78-3.
IACS, 2006a. Common Structural Rules for Bulk Carriers. International Association of Classification Societies, London, UK.
IACS, 2006b. Common Structural Rules for Double Hull Oil Tankers. International Association of Classification Societies, London, UK.
ISSC, 2009. Ultimate Strength (Committee III.1), The 17th International Ship and Offshore Structures Congress (ISSC 2009), 16-21 August, Seoul, Korea.
ISSC, 2012. Ultimate Strength (Committee III.1), The 18th International Ship and Offshore Structures Congress

(ISSC 2012), 9-13 September, Rostock, Germany.
ISSC, 2015. Ultimate Strength (Committee III.1), The 19th International Ship and Offshore Structures Congress (ISSC 2015), 7-10 September, Cascais, Portugal.
ISSC, 2018. Ultimate Strength (Committee III.1), The 20th International Ship and Offshore Structures Congress (ISSC 2018), 9-13 September, Liege, Belgium & Amsterdam, The Netherlands.
ISSC, 2022. Ultimate Strength (Committee III.1), The 21th International Ship and Offshore Structures Congress (ISSC 2022), 10-16 September, Vancouver, Canada.
Ivanov, L.D., Rousev, S.G., 1979. Statistical estimation of reduction coefficient of ship's hull plates with initial deflections. The Naval Architect (4), 158-160.
Jiang, L., Zhang, S., 2015. Lateral Pressure Effects on the Ultimate Strength of Plates, ASME 2015 34th International Conference on Ocean, Offshore and Arctic Engineering.
Jiang, L., Zhang, S., 2021. Effect of pressure on collapse behavior of stiffened panel, Developments in Maritime Technology and Engineering. CRC Press.
Kee Paik, J., Kyun Kim, D., Lee, H., Lae Shim, Y., 2011. A Method for Analyzing Elastic Large Deflection Behavior of Perfect and Imperfect Plates With Partially Rotation-Restrained Edges. Journal of Offshore Mechanics and Arctic Engineering 134 (2).
Khan, I., Zhang, S., 2011. Effects of welding-induced residual stress on ultimate strength of plates and stiffened panels. Ships and Offshore Structures 6 (4), 297-309.
Khedmati, M.R., Memarian, H.R., Fadavie, M., Zareei, M.R., 2016. Empirical formulations for estimation of ultimate strength of continuous aluminium stiffened plates under combined transverse compression and lateral pressure. Ships and Offshore Structures 11 (3), 258-277.
Khedmati, M.R., Zareei, M.R., Rigo, P., 2010. Empirical formulations for estimation of ultimate strength of continuous stiffened aluminium plates under combined in-plane compression and lateral pressure. Thin-Walled Structures 48 (3), 274-289.
Kim, D.K., 2013. Condition Assessment of Damaged Ships and Ship-shaped Offshore Structures, Ph.D. Dissertation. Pusan National University, Busan, Korea.
Kim, D.K., Kim, H.B., Zhang, X., Li, C.G., Paik, J.K., 2014. Ultimate strength performance of tankers associated with industry corrosion addition practices. International Journal of Naval Architecture and Ocean Engineering 6 (3), 507-528.
Kim, D.K., Kim, S.J., Kim, H.B., Zhang, X.M., Li, C.G., Paik, J.K., 2015. Ultimate strength performance of bulk carriers with various corrosion additions. Ships and Offshore Structures 10 (1), 59-78.
Kim, D.K., Li, S., Lee, J.R., Poh, B.Y., Benson, S., Cho, N.-K., 2022. An empirical formula to assess ultimate strength of initially deflected plate:
Part 1 = Propose the general shape and application to longitudinal compression. Ocean Engineering, Under Revision.
Kim, D.K., Lim, H.L., Kim, M.S., Hwang, O.J., Park, K.S., 2017. An empirical formulation for predicting the ultimate strength of stiffened panels subjected to longitudinal compression. Ocean Engineering 140, 270-280.
Kim, D.K., Lim, H.L., Yu, S.Y., 2018a. A technical review on ultimate strength prediction of stiffened panels in axial compression. Ocean Engineering 170, 392-406.
Kim, D.K., Lim, H.L., Yu, S.Y., 2019a. Ultimate strength prediction of T-bar stiffened panel under longitudinal compression by data processing: A refined empirical formulation. Ocean Engineering 192, 106522.
Kim, D.K., Park, D.K., Kim, J.H., Kim, S.J., Kim, B.J., Seo, J.K., Paik, J.K., 2012. Effect of corrosion on the ultimate strength of double hull oil tankers- Part I: stiffened panels. Structural Engineering and Mechanics 42 (4), 507-530.
Kim, D.K., Poh, B.Y., Lee, J.R., Paik, J.K., 2018b. Ultimate strength of initially deflected plate under longitudinal compression: Part I = An advanced empirical formulation. Structural Engineering and Mechanics 68 (2), 247-259.
Kim, D.K., Wong, E.W.C., Lee, E.B., Yu, S.Y., Kim, Y.T., 2019b. A method for the empirical formulation of current profile. Ships and Offshore Structures 14 (2), 176-192.
Kim, D.K., Yu, S.Y., Lim, H.L., Cho, N.-K., 2020. Ultimate compressive strength of stiffened panel: An empirical formulation for flat-bar type. Journal of Marine Science and Engineering 8 (8), 605.
Kim, J.-H., Park, D.-H., Kim, S.-K., Kim, M.-S., Lee, J.-M., 2021. Experimental Study and Development of Design Formula for Estimating the Ultimate Strength of Curved Plates. Applied Sciences 11 (5).
Kong, X., Yang, Y., Gan, J., Yuan, T., Ao, L., Wu, W., 2020. Experimental and numerical investigation on the detailed buckling process of similar stiffened panels subjected to in-plane compressive load. Thin-Walled Structures 148, 106620.

Li, S., Georgiadis, D.G., Kim, D.K., Samuelides, M.S., 2022. A comparison of geometric imperfection models for collapse analysis of ship-type stiffened plated grillages. Engineering Structures 250, 113480.
Li, S., Hu, Z., Benson, S., 2019. An analytical method to predict the buckling and collapse behaviour of plates and stiffened panels under cyclic loading. Engineering Structures 199, 109627.
Li, S., Kim, D., Benson, S., 2021a. An adaptable algorithm to predict the load-shortening curves of stiffened panels in longitudinal compression. Ships Offshore Struct., In-press (Availble: https://doi.org/10.1080/17445302.17442021.17445319).
Li, S., Kim, D.K., 2022. Ultimate strength characteristics of unstiffened cylindrical shell in axial compression. Ocean Engineering 243, 110253.
Li, S., Kim, D.K., Benson, S., 2021b. The influence of residual stress on the ultimate strength of longitudinally compressed stiffened panels. Ocean Engineering, 108839.
Li, S., Kim, D.K., Benson, S., 2021c. A probabilistic approach to assess the computational uncertainty of ultimate strength of hull girders. Reliability Engineering & System Safety 213, 107688.
Lim, H.L., 2018. A study on development of refined empirical formulation in predicting the ultimate strength of stiffened panel subjected to longitudinal compression, Department of Civil and Environmental Engineering. Universiti Teknologi PETRONAS, Perak, Malaysia.
Lind, N.C., Ravindra, M.K., Power, J., 1971. A review of the effective width formula, The 1st International Specialty Conference on Cold-Formed Steel Structures. University of Missouri--Rolla.
Liu, B., Doan, V.T., Garbatov, Y., Wu, W., Guedes Soares, C., 2020. Study on Ultimate Compressive Strength of Aluminium-Alloy Plates and Stiffened Panels. Journal of Marine Science and Application 19 (4), 534-552.
Ma, H., Wang, D., 2021. Lateral pressure effect on the ultimate strength of the stiffened plate subjected to combined loads. Ocean Engineering 239, 109926.
Ma, H., Xiong, Q., Wang, D., 2021. Experimental and numerical study on the ultimate strength of stiffened plates subjected to combined biaxial compression and lateral loads. Ocean Engineering 228, 108928.
Manuel Gordo, J., Guedes Soares, C., 2011. Compressive Tests on Long Continuous Stiffened Panels. Journal of Offshore Mechanics and Arctic Engineering 134 (2), 021403.
Marguerre, K., 1937. Die mittragende Breite der gedrückten Platte. Translated NACA Technical Note 833 (in German) & Luftfahrtforschung (Original) 14 (3), 121-128.
Oh, D., Race, J., Oterkus, S., Koo, B., 2020. Burst pressure prediction of API 5L X-grade dented pipelines using deep neural network. Journal of Marine Science and Engineering 8 (10), 766.
Paik, J.K., 2007. Empirical formulations for predicting the ultimate compressive strength of welded aluminum stiffened panels. Thin-Walled Structures 45 (2), 171-184.
Paik, J.K., 2008. Some recent advances in the concepts of plate-effectiveness evaluation. Thin-Walled Structures 46 (7), 1035-1046.
Paik, J.K., 2018. Ultimate limit state analysis and design of plated structures (2nd Ed.). John Wiley & Sons, Chichester, UK.
Paik, J.K., Kim, B.J., Seo, J.K., 2008a. Methods for ultimate limit state assessment of ships and ship-shaped offshore structures: Part I—Unstiffened plates. Ocean Engineering 35 (2), 261-270.
Paik, J.K., Kim, B.J., Seo, J.K., 2008b. Methods for ultimate limit state assessment of ships and ship-shaped offshore structures: Part II stiffened panels. Ocean Engineering 35 (2), 271-280.
Paik, J.K., Kim, B.J., Seo, J.K., 2008c. Methods for ultimate limit state assessment of ships and ship-shaped offshore structures: Part III hull girders. Ocean Engineering 35 (2), 281-286.
Paik, J.K., Kim, D.K., Kim, M.S., 2009. Ultimate strength performance of Suezmax tanker structures: pre-CSR versus CSR designs. International Journal of Maritime Engineering 151 (Part A2), 39-58.
Paik, J.K., Lee, D.H., Noh, S.H., Park, D.K., Ringsberg, J.W., 2020. Full-scale collapse testing of a steel stiffened plate structure under cyclic axial-compressive loading. Structures 26, 996-1009.
Paik, J.K., Seo, J.K., 2009a. Nonlinear finite element method models for ultimate strength analysis of steel stiffened-plate structures under combined biaxial compression and lateral pressure actions—Part I: Plate elements. Thin-Walled Structures 47 (8), 1008-1017.
Paik, J.K., Seo, J.K., 2009b. Nonlinear finite element method models for ultimate strength analysis of steel stiffened-plate structures under combined biaxial compression and lateral pressure actions—Part II: Stiffened panels. Thin-Walled Structures 47 (8), 998-1007.
Paik, J.K., Thayamballi, A.K., 1997. An Empirical Formulation For Predicting the Ultimate Compressive Strength of Stiffened Panels, The 7th International Offshore and Polar Engineering Conference (ISOPE 1997), 25-30 May, Honolulu, Hawaii, USA, pp. ISOPE-I-97-444.

Paik, J.K., Thayamballi, A.K., Lee, J.M., 2004. Effect of initial deflection shape on the ultimate strength behavior of welded steel plates under biaxial compressive loads. Journal of Ship research 48 (1), 45-60.
Raviprakash, A.V., Prabu, B., Alagumurthi, N., 2012. Residual ultimate compressive strength of dented square plates. Thin-Walled Structures 58, 32-39.
Ringsberg, J.W., Darie, I., Nahshon, K., Shilling, G., Vaz, M.A., Benson, S., Brubak, L., Feng, G., Fujikubo, M., Gaiotti, M., Hu, Z., Jang, B.-S., Paik, J.-K., Slagstad, M., Tabri, K., Wang, Y., Wiegard, B., Yanagihara, D., 2021. The ISSC 2022 committee III.1-Ultimate strength benchmark study on the ultimate limit state analysis of a stiffened plate structure subjected to uniaxial compressive loads. Marine Structures 79, 103026.
Sadovský, Z., Teixeira, A.P., Guedes Soares, C., 2005. Degradation of the compressive strength of rectangular plates due to initial deflection. Thin-Walled Structures 43 (1), 65-82.
Salazar-Domínguez, C.M., Hernández-Hernández, J., Rosas-Huerta, E.D., Iturbe-Rosas, G.E., Herrera-May, A.L., 2021. Structural Analysis of a Barge Midship Section Considering the Still Water and Wave Load Effects. Journal of Marine Science and Engineering 9 (1).
Schnadel, G., 1930. Die Uberschreitung der Knickgrenze bei dunnen Platlen, Proceedings of the 3rd International Congress for Applied Mechanics Stockholm, Sweden, p. 73.
Sechler, E.E., 1933. The ultimate strength of thin flat sheets in compression. Guggenheim Aeronautical Laboratory (Publication 27), California Institute of Technology, Pasadena, CA, USA.
Shanmugam, N.E., Dongqi, Z., Choo, Y.S., Arockiaswamy, M., 2014. Experimental studies on stiffened plates under in-plane load and lateral pressure. Thin-Walled Structures 80, 22-31.
Smith, C.S., Davidson, P.C., Chapman, J.C., Dowling, P.J., 1988. Strength and stiffness of ships'plating under in-plane compression and tension. Royal Institution of Naval Architects Transactions 130, 277-296.
Soreide, T.H., Czujko, J., 1983. Load carrying capacities of plates under combined lateral load and axial/biaxial compression, The 2nd International Symposium on Practical Design in Shipbuilding (PRADS 1983), 17-22 October, Tokyo and Seoul, Japan and Korea.
Timoshenko, S.P., 1936. Theory of elastic stability. McGraw-Hill New York, NY, USA.
Ueda, Y., Rashed, S.M., Paik, J.K., 1986. Effective width of rectangular plates subjected to combined loads. Journal of the Society of Naval Architects of Japan 1986 (159), 258-270.
Ueda, Y., Yao, T., Nakacho, K., Yuan, M.G., 1992. Prediction of welding residual stress, deformation and ultimate strength of plate panels. Transactions of the JWRI (Japan Welding Research Institute) (Japan) 21 (2), 137-143.
Ueda, Y., Yasukawa, W., Yao, T., Ikegami, H., Ominami, R., 1975. Ultimate strength of square plates subjected to compression (1st Report). Journal of the Society of Naval Architects of Japan 1975 (137), 210-221.
von Kármán, T., 1924. Die mittragende breite (The effective width), Beiträge zur Technischen Mechanik und Technischen Physik (in German). Springer, pp. 114-127.
Winter, G., 1940. Stress Distribution in and Equivalent Width of Flanges of Wide, Thin-Wall Steel Beams, National Advisory Committee for Aeronautics (NACA) Cornell University, Washington DC, USA.
Wong, E.W.C., Kim, D.K., 2018. A simplified method to predict fatigue damage of TTR subjected to short-term VIV using artificial neural network. Advances in Engineering Software 126, 100-109.
Xu, M., Soares, C.G., 2012. Assessment of the ultimate strength of narrow stiffened panel test specimens. Thin-Walled Structures 55, 11-21.
Xu, M.C., Song, Z.J., Pan, J., Soares, C.G., 2017. Ultimate strength assessment of continuous stiffened panels under combined longitudinal compressive load and lateral pressure. Ocean Engineering 139, 39-53.
Xu, M.C., Song, Z.J., Zhang, B.W., Pan, J., 2018. Empirical formula for predicting ultimate strength of stiffened panel of ship structure under combined longitudinal compression and lateral loads. Ocean Engineering 162, 161-175.
Yao, T., Fujikubo, M., 2016a. Buckling and ultimate strength of ship and ship-like floating structures. Butterworth-Heinemann.
Yao, T., Fujikubo, M., 2016b. Chapter 2 - Initial Imperfections due to Welding, in: Yao, T., Fujikubo, M. (Eds.), Buckling and Ultimate Strength of Ship and Ship-Like Floating Structures. Butterworth-Heinemann, pp. 13-34.
Zhang, S., 2016. A review and study on ultimate strength of steel plates and stiffened panels in axial compression. Ships and Offshore Structures 11 (1), 81-91.